RESEARCH, DEVELOPMENT
AND
FABRICATION OF LITHIUM SOLAR CELLS
FINAL REPORT, PART II

April 1972

JPL CONTRACT NO. 952546

Jet Propulsion Laboratory
California Institute of Technology
4800 Oak Grove Drive
Pasadena, California 91103

Prepared by
Peter A. Iles

Centralab Semiconductor Division
GLOBE-UNION, INC.
4501 N. Arden Drive
El Monte, California 91734

RESEARCH, DEVELOPMENT
AND
FABRICATION OF LITHIUM SOLAR CELLS
FINAL REPORT, PART II

April 1972

JPL CONTRACT NO. 952546

Jet Propulsion Laboratory
California Institute of Technology
4800 Oak Grove Drive
Pasadena, California 91103

Prepared by
Peter A. Iles

Centralab Semiconductor Division
GLOBE-UNION, INC.
4501 N. Arden Drive
El Monte, California 91734

RESEARCH, DEVELOPMENT & FABRICATION

OF

LITHIUM SOLAR CELLS

FINAL REPORT, PART II

FROM

CENTRALAB SEMICONDUCTOR DIVISION

UNDER

JPL CONTRACT 952546

This work was performed for the Jet Propulsion Laboratory, California Institute of Technology, as sponsored by the National Aeronautics and Space Administration under Contract NAS 7-100.

This report contains information prepared by Centralab Semiconductor, a Division of Globe-Union Inc., under JPL Subcontract No. 952546.

Its content is not necessarily endorsed by the Jet Propulsion Laboratory, California Institute of Technology or the National Aeronautics and Space Administration.

ABSTRACT

The remaining work on this contract was concentrated on study of several single-step, lithium diffusion schedules using lower temperatures (330°C to 370°C) and times in the range from 2 hours to 8 hours. Previously developed improved boron diffusion methods were maintained. A detailed comparison was made using evaporated lithium metal as the lithium source, and greatly improved consistency in lithium concentrations was obtained. It was possible to combine all processing steps to obtain lithium doped cells of high output which also contained adequate lithium to ensure good recoverability. In this reporting period 1290 cells were shipped, and their properties are summarized. Recommendations are made for future work.

TABLE OF CONTENTS

LIST OF TABLES

LIST OF FIGURES

1.0 Summary

This report completes the final report on a program to develop lithium doped silicon solar cells giving performance in space superior to N/P cells.

The cells are better understood and have been further improved by better process control, including combining the improved boron diffusion methods developed earlier with better lithium diffusion techniques. Also, better analytical methods provided quantitative guidance in optimizing these steps, and in arranging the fabrication sequence to provide cells with both higher output and containing adequate concentrations of lithium with close tolerances on the spread within batches. These analytical methods included the use of I-V cell characteristics and analysis of the capacitance-voltage relations near the cell PN junction. The overall control has improved to allow more precise predictions for the various photovoltaic parameters, and the procedures can be adjusted to suit the oxygen concentration of the silicon.

The trend to moderate single-cycle lithium diffusions was guided by feedback from the irradiation groups and by the good initial performance of the cells. Spreading resistance probe measurements, complemented by capacitance analysis, showed diffusion conditions where the lithium source was not adequate during longer time diffusions, and in turn led to improved control. Figures 17 through 24 show the increased control of lithium near the PN junction, and after extensive analysis the present JPL program has shown that the lithium in this region controls most of the properties of lithium cells.

Twelve hundred ninety cells were shipped. A summary of the I-V characteristics is given in Table 5 and shows the general high level of cell output, particularly the improvement of curve shape (shown by increased CPF), and the lithium concentrations achieved.

A recommendation is made that lithium cells are sufficiently promising for work to continue on scaling-up the key processes.

Note: Work performed subsequent to this contract has shown that the level of control achieved was maintained for reasonably large numbers of cells and that the average output (for the same lithium concentrations) can be further increased.

2.0 Introduction

The aim is to develop high efficiency radiation-tolerant solar cells using lithium doping to improve cell output after irradiation. This contract continues work on controlling the cell fabrication procedures to determine the major control steps and means for monitoring these steps. The procedures developed are combined to give closely controlled groups of cells which other organizations can irradiate and analyze.

Exchange of information via JPL, concerning the control of the fabrication steps and the results of irradiation analysis, allowed specification of later cell groups.

The work described here builds on that already done (Refs. 1 & 2). Thus, the emphasis is still on lithium diffusion temperatures below 400°C, with single-cycle diffusion rather than redistribution cycles. In addition, the key fabrication steps were evaluated in terms of scaling-up to pilot production levels.

3.0 Technical Discussion

3.1 Silicon

Previous reports described the differences in cell behavior between oxygen-rich (OR) and oxygen-lean (OL) silicon, following identical boron and lithium diffusions. Last report (Ref. 1) outlined how the use of boron diffusion methods, introducing less strain in the silicon, allowed the performance of cells with OL silicon to approach that of OR silicon.

There are still minor differences in the lithium distribution in the two forms of silicon, and more study is needed to identify the physical reasons for this.

Of the 1290 cells shipped in this period, 180 used OL silicon and 1110 used OR silicon. The differences in post-irradiation behavior between the two forms of silicon have been well established by irradiation groups. In general, for mission temperatures exceeding 60°C and moderate fluences, OR silicon is preferred at present; for lower temperatures, or where faster recovery rates are needed, OL silicon is preferable.

3.2 Boron Diffusion Methods

The modified BCl_3 schedules (principally the reduced tack-on times or low flow rates developed by Centralab earlier in this contract) have consistently provided the cells with best controlled properties and the highest output. These diffusion methods were used for the present phase, which concentrated on supplying

reasonably large groups covering a matrix selection of lithium diffusion cycles with some variations in silicon resistivity and form, and in the method of depositing lithium.

3.3 Lithium Doping

3.3.1 Sources of Lithium

During this reporting period, only two sources of lithium have been used, namely paint-on of lithium aluminum hydride and vacuum evaporation of lithium metal. The I-V characteristics obtained using either source are comparable. However, it was found during this phase of the work (see Section 3.5.1 below) that for long duration cycles, even at low temperatures, the paint-on method did not produce an unlimited concentration of lithium and there was a consequent spread in lithium concentration gradient.

Better control of the evaporation method was achieved, resulting in greater consistency of lithium concentration near the PN junction, and also of cell properties, especially after irradiation. The greater control was obtained by improving the following aspects of the evaporation method. The lithium source boat geometry was improved, and with the use of a cooled substrate supporting the silicon slices, led to greater uniformity in the deposited lithium layers. Also, the use of inert gas flushing to raise the evaporation chamber pressure, and keeping the slices in an inert enclosure to reduce lithium interaction enroute to the diffusion furnace, allowed exploitation of the deposition improvements. These improvements were not all realized immediately, but it was noticeable that as experience was gained, the overall control of lithium distributions improved for the later shipment groups, as will be seen in Section 3.5 below.

3.3.2 Lithium Distribution

In reference 1, a detailed description was given of the lithium distribution near both the back surface and the front P+ layer for a range of single temperature-time drive-in cycles. Traveling probe measurements were used to explore the donor concentration in the bulk and near the back surface. The slices were sectioned and the spatial resistivity values were obtained from a calibrated moveable resistance probe. Analysis of the capacitance-reverse voltage behavior of the cell allowed calculation of both the donor concentration and the concentration gradient near the PN junction.

In the present work, most reliance was placed on capacitance measurements because detailed analysis by irradiation groups (see Refs. 3 & 4) had shown that most of the pre- and post-irradiation properties of lithium cells could be predicted from knowledge of the lithium concentration near the PN junction.

In the summaries of the shipped groups given below, estimates of donor concentration (or an associated estimate using capacitance values) are given in all cases and are the most sensitive indicators of the degree of lithium control achieved.

More information and insight has been added to the way in which the lithium is distributed and the resultant effects on cell properties.

Surface Concentration (C_s). The buildup of the lithium concentration at the back surface where the lithium was applied, was measured as a function of time at various temperatures.

Figure 1 shows the measured values. Qualitatively the results are as expected, with a gradual buildup of C_s for longer times to a maximum value--the rate of increase and the maximum value being higher for higher temperatures.

Two other features are noted. First, the buildup was slower than expected, often requiring around one hour to reach the maximum C_s value. Second, after the saturation region, C_s decreased for longer diffusion times. The points shown in Figure 1 for times greater than two hours are those calculated for the C-13 cells discussed in Section 3.5.1 below.

Concentration Near the PN Junction. Theoretically, both the lithium concentration and its gradient at any plane in the cell, including the important region near the PN junction at the front of the cell, are both directly proportional to C_s. However, the lithium concentration gradient near the junction must be much increased over the theoretical value in order to give concentrations which agree with those calculated from C-V measurements. Gradients up to seven times the theoretical value have been measured. The cause of this increase and the associated lower concentration at the junction are believed to be the perturbation of the theoretical lithium distribution by the electric field in the junction depletion region which assists the flow of lithium into the P+ layer.

The changes in lithium distribution were studied by measurements on samples diffused at a given temperature for several different times. Figure 2 shows the results of such a test. The lithium buildup at the PN junction was followed by capacitance measurements. For the three shorter times, no measurable increase at the junction was observed, in keeping with the theoretical curves shown. The two longer times are seen to give increases in lithium near the junction. The changes needed in the theoretical distribution are shown by the dotted lines.

Good consistency between measured and theoretical lithium distributions was obtained by the dotted line portions, if these portions took place over approximately 20μm from the PN junction.

Changes in Concentration with Diffusion Time The trend noted above for the C_s value, at a given temperature to decrease steadily with diffusion time, gave increased spread in C_s values. This in turn led to increased spread towards lower value of lithium concentrations and gradient near the junction. Although the cause of these changes was first sought in leakage effects near the junction, the C_s measurements showed that the likely cause was the decrease in C_s resulting from depletion of the lithium source.

This depletion could be reduced by controlling the amount of lithium deposited or by modification of the diffusion procedure to minimize losses. In discussion of C-15 below, the cell parameters resulting from wide variation in C_s are compared to the tighter grouping obtained when the lithium source depletion was reduced.

3.4 Fabrication Sequence

For the present tests, the surface finish of the slices was kept constant. This meant that the front surface was mechanically-chemically polished and the back side was of rough finish (as sawn) but etched lightly. Associated tests showed that it was possible to fabricate good cells with a highly polished back surface, and also that good performance cells could be obtained when aluminum contacts were used for both the front and back surfaces.

As mentioned above, the boron diffusion methods developed by Centralab last year (reduced tack-on cycles with BCl_3) were maintained because they gave well controlled cells of good output with both oxygen-rich and oxygen-lean silicon, and thus allowed the variables of the lithium introduction to be examined in more detail.

The search for greater consistency of cell fabrication continued. The various fabrication steps interact and their order of performance is important.

For example, previously the front surface contact and coating were in place before the lithium was introduced, thus allowing a more severe sintering cycle to be used. However, there was the chance of attack of the contact and coating by the lithium during its application and diffusion. In the later groups of cells a larger scale test was made of the sequence where the front surface contact and coating were applied after lithium diffusion. The cells showed good consistency of I-V properties and adequate adhesion with the use of moderate

sinter cycles at temperatures below those used for lithium diffusion. There was a noticeable increase in curve power factor (CPF) for the later groups fabricated (see Table 5).

Also, it was possible to leave a boron-silicon compound on the P+ layer during lithium diffusion, a factor favorable to use of the lithium metal evaporation process. The use of the lower lithium diffusion temperatures also helped to minimize interaction of lithium with the cell front surface.

3.5 Cell Shipments

The number sequence from last year's shipments was continued.

3.5.1 JPL Shipment C-13

This shipment was intended to extend the work described in Reference 1, Section 3.3.1, which described five separate temperature-time sequences (425°C - 90 min., 400°C - 90 min., 375°C - 180 min., 350°C - 300 min., and 325°C - 480 min.).

For C-13, five temperatures were chosen - namely, 330°C, 340°C, 350°C, 360°C & 370°C. At each temperature, two separate diffusion time groups were used as shown in Table 1. The times for the two 350°C diffusions were identical (300 min.) and were carried out at the beginning and end of the sequence to check repeatability of the same sequence.

All cells fabricated were from the same OR ingot. Also, the slices all had the same surface finish (chemical-mechanical polish) and the same boron diffusion schedule. (BCl_3 with short (4 min.) tack-on time).

The slices were all boron diffused before further processing. By mistake, the BCl_3 temperature was 20°C high for the first 30% of the slices diffused (groups 13E, 13I, 13J). This led to a deeper PN junction, but close examination of the final cells showed that this deeper junction did not have significant effect on any cell parameters except the expected difference - a loss of 2-3mA in short circuit current. This loss was in short wavelength response and agreed with earlier tests wherein the boron diffusion schedule was varied intentionally. The two groups of cells processed at 350°C (F and E) were diffused at these two boron temperatures - 1050°C and 1070°C - and later results show that apart from I_{sc} variations, they are fairly well matched. Therefore, in comparing these ten groups the three groups with deeper junctions (13E, 13I, 13J) had the measured I_{sc} adjusted upwards by 2.5mA.

TABLE 1

Lithium Diffusion Schedules Used For Shipment C-13

(Lithium Paint-On)

Group	No. of Cells	Diffusion Temperature	Diffusion Time
13A	30	330°C	180 min.
13B	30	330°C	420 min.
13C	30	340°C	180 min.
13D	30	340°C	420 min.
13E	30	350°C	300 min.
13F	30	350°C	300 min.
13G	30	360°C	180 min.
13H	30	360°C	420 min.
13I	30	370°C	240 min.
13J	30	370°C	360 min.

The lithium diffusion schedules used are shown in Table 1. At each diffusion temperature the lithium was applied to batches of slices and the diffusion was performed on a split boat, allowing withdrawal of the shorter time group first, leaving the longer time group in the furnace. The differences in cell properties for both short and long time diffusions were batch-dependent rather than time-dependent, showing that the main variable was in the paint-on lithium application. The fabrication sequence applied front contacts and coating before lithium diffusion.

In general, the cells showed good control and good I-V performance. The controlling variable was the diffusion time. Figure 3 shows the average values of Pmax, V_{oc}, I_{sc} and capacitance for the thirty-cell groups in C-13. Pmax values are high and well grouped, and vary about 4%. V_{oc} and I_{sc} show slightly larger ranges (up to 5.5%) but their out-of-phase variations led to reduced spread in Pmax. Also, V_{oc} and capacitance vary in phase, the spread in capacitance being up to 30%.

Figures 4 and 5 show in more detail some of the parameters for the C-13 groups. In these figures, average values and the spread in the groups for Pmax, V_{oc}, capacitance and donor concentration values near the junction, are plotted as a function of increasing diffusion time. The Pmax. values are satisfactorily high and tightly grouped. The other parameters all show a trend toward lower values and larger spreads at the longer times. These two figures show that the I-V characteristics can have small spread, but may be associated with larger spread in the lithium concentration or its gradient.

Figure 6 plots the cumulative percentage of Pmax, averaged for all 300 cells in C-13, with the upper and lower 30 cell groups shown also. For comparison, the distribution for C-12 is given. This figure shows that the general level of cell output was good.

Figure 7, for ten cells in C-13G and C-13H, shows good correlation between V_{oc} and the lithium concentration and concentration gradient near the junction, calculated from capacitance measurements. For C-13G, the shorter time diffusion, the grouping is tighter and both V_{oc} and the lithium parameters are higher. Even for cells with less lithium the V_{oc} values are generally high, and this figure shows that greater resolution of the underlying correlations is now feasible.

Figure 8, plotted for 100 cells (10 in each C-13 group) shows that V_{oc} is approximately proportional to the logarithm of the lithium concentration. The estimated slope of the curve is approximately 0.026 $volt^{-1}$, a value expected if the PN junction is operating at current levels where it approaches diode diffusion theory operation. The total spread in V_{oc} is around 5%, whereas the total spread in concentration is 400%.

Table 2 lists the values of surface concentration calculated for each of the C-13 groups. These C_s values were obtained by combining the lithium concentration and concentration gradient near the PN junction (estimated from C-V methods). Assuming the gradient occurred for a distance of 20μm from the junction, a value of lithium concentration was obtained at this 20μm plane. Then the theoretical distribution was extrapolated from this plane to the back surface to give the C_s value. The groups in Table 2 are plotted in increasing order of diffusion time, and show the steady fall-off of C_s.

In summary, C-13 provided 300 cells of good output but with sufficient differences between the groups to show that diffusion time was a more important controlling parameter than had been suspected earlier. To reduce the effects of source depletion at the longer times, a later shipment (C-15) was planned to include both paint-on and evaporated sources to check that the source depletion was reduced for the more concentrated source.

3.5.2 JPL Shipment C-14

The intention in C-14 was to compare oxygen-rich (CG) silicon and oxygen-lean (Lopex) silicon in two of the lower temperature single-time cycles. Also, lower resistivity Lopex silicon (15 ohm/cm) was used to check if the five-fold increase in background concentration was of advantage for higher fluence irradiations. The fabrication sequence for C-14 applied lithium before any contacts or coatings were present. Table 3 gives details of the silicon and lithium cycles used.

Figure 9 gives the average values and the spread of Pmax, V_{oc} and capacitance for the C-14 groups. The general level of Pmax and V_{oc} was good. For a given lithium cycle, theCG silicon cells had higher V_{oc} and I_{sc} than the Lopex cells. However, this higher V_{oc} was accompanied by the lower capacitance (thus lower lithium concentration near the junction) usually found for CG silicon. This lower capacitance can explain the higher I_{sc} values obtained for CG silicon, but does not explain the V_{oc} differences. In this case, the differences in silicon grown by the two methods have more effect on I-V characteristics than the differences obtained in lithium concentration. Figure 10 plots the cumulative percentage of Pmax for C-14 cells.

3.5.3 JPL Shipment C-15

The purpose of C-15 was to compare three different silicon ingots (OL 15 ohm/cm, OL 75 ohm/cm, OR 30 ohm/cm) all diffused for the same schedule, 350°C - 240 min. Each group of the three ingots was split, with lithium being

TABLE 2

Surface Concentration of Lithium for C-13 Groups

Combined the lithium concentration at the PN junction and the measured lithium concentration gradient near the junction, assumed to be spread over 20 μm.

Also assumed complementary error function distribution.

Group	T(°C)	t(min)	Calculated C_s (cm^{-3})
13A	330	180	1.3×10^{17}
13C	340	180	1.7×10^{17}
13G	360	180	1.6×10^{17}
13I	370	240	0.95×10^{17}
13E	350	300	1.2×10^{17}
13F	350	300	1.2×10^{17}
13J	370	360	0.75×10^{17}
13B	330	420	0.7×10^{17}
13D	340	420	0.5×10^{17}
13H	360	420	0.65×10^{17}

Table 3. Details of JPL Shipment C-14.

Cell Group	No. of Cells	Silicon Used	Lithium Diffusion
C-14A	30	Lopex - 15 ohm-cm	Paint-on 375°C - 180 min.
C-14B	30	C G - 30 ohm-cm	Paint-on 375°C - 180 min.
C-14C	30	Lopex - 15 ohm-cm	Paint-on 350°C - 300 min.
C-14D	30	C G - 30 ohm-cm	Paint-on 350°C - 300 min.

Table 4. Details of JPL Shipment C-15.

Cell Group	No. of Cells	Silicon Used	Lithium Diffusion
C-15A	30	Lopex - 15 ohm-cm	Paint-on 350°C - 240 min.
C-15B	30	Lopex - 15 ohm-cm	Evaporated 350°C - 240 min.
C-15C	30	Lopex - 75 ohm-cm	Paint-on 350°C - 240 min.
C-15D	30	Lopex - 75 ohm-cm	Evaporated 350°C - 240 min.
C-15E	30	CG - 30 ohm-cm	Paint-on 350°C - 240 min.
C-15F	30	CG - 30 ohm-cm	Evaporated 350°C - 240 min.
C-15G	30	CG - 30 ohm-cm	Evaporated 350°C - 480 min.

painted-on half the groups and lithium metal being evaporated on the other half. This provided a good comparison of the control possible with these two lithium techniques. Comparison was made between the two OL ingots with five-fold doping difference. In addition, a seventh group used OR silicon as above and evaporated lithium, with a diffusion schedule 350°C - 480 min., to study the effects of the longer time with the more concentrated lithium source.

Table 4 shows details of the C-15 groups.

Figure 11 plots the average values and the spread for the various C-15 groups. Again, the overall level of Pmax is good and as seen in C-11 and C-14, the Pmax values for CG silicon are slightly higher than those for Lopex cells. There is no significant difference in these pre-irradiation measurements between the medium and high resistivity Lopex groups. Also, as for C-14, the lithium concentration near the PN junction, as measured by capacitance, was higher for the Lopex ingots.

The overall spread is not markedly lower for the lithium evaporation groups, possibly because the diffusion time is not long. However, the spread in Pmax and especially in capacitance for the eight hour diffusion group C-15G was much lower than obtained for the longer time C-13 groups. This shows that lithium depletion has been minimized by the more concentrated source.

During fabrication of the evaporated lithium groups, some batches showed signs of severe lithium depletion. These signs included both serious reduction in V_{oc} (with accompanying higher I_{sc}) and low capacitance values often near the level found for cells made with no lithium. Resistance probe measurements showed that the lithium concentration was much reduced for these batches. These tests showed that lithium evaporation was technique dependent. The interaction between lithium and silicon was reduced by maintaining the slices in an inert atmosphere up to the stage where they were placed in the diffusion furnace. This gave increased lithium concentrations with very closely grouped sets of parameters. Figure 12 compares the spread of three cell parameters, V_{oc}, capacitance and Pmax for three different conditions of lithium application--namely paint-on, lithium evaporation with varying interaction and well controlled lithium evaporation. The silicon used for these three tests was the same (Lopex, 75 ohm/cm) as was the lithium diffusion schedule 350°C - 240 min. The paint-on source again shows tight grouping of Pmax and V_{oc} with a wider spread in capacitance. The less controlled evaporation group had lower values for Pmax, V_{oc}, and capacitance with wide spreads. The well controlled evaporation group had high values with small spread for all parameters. The lithium diffusion techniques used for the well

controlled groups in C-15 were used for the later cell groups (C-16 through C-18) and gave tighter control of the lithium distribution.

Figure 13 shows the cumulative percentage of Pmax for the C-15 cells.

3.5.4 JPL Shipment C-16

Two relatively large groups (180 cells in each group) of OR silicon, 20 ohm/cm were made using evaporated lithium and a moderate diffusion schedule (370°C - 180 min.), to check consistency in scaling-up. One group (C-16A) had solder-covered contacts.

The values for Pmax, zero-bias capacitance (Co) and donor concentration (Nd) are given in Figure 14.

Figure 15 gives the cumulative percentage of Pmax for C-16 cells.

3.5.5 JPL Shipment C-17

A lower resistivity OR ingot (10 ohm/cm) was used with the same lithium conditions as for C-16. Figure 14 also summarizes Pmax, Co and Nd for these cells. Figure 15 shows the cumulative Pmax distribution.

3.5.6 JPL Shipment C-18

Three groups were fabricated from 20 ohm/cm OR silicon with evaporated lithium schedules 350°C - 120 min., 360°C - 120 min., and 370°C - 120 min. Figure 14 shows the Pmax, Co and Nd values, and also shows the greater control achieved over Co and Nd. The cumulative Pmax distribution is also given in Figure 15.

3.6 Comments on Cell Shipments

Most of the moderate lithium diffusion schedules used in this phase have resulted in good I-V characteristics (I_{sc}, V_{oc}, and Pmax), with tight grouping. The spread observed in I_{sc} and V_{oc} could be related directly to the variations in lithium concentration.

Table 5 summarizes the median values for the I-V characteristics and zero-bias capacitance for all cell groups described in this report. In addition to emphasizing some of the comments given above in discussing the various groups, attention is drawn to the gradual increase in curve power factor (CPF) resulting from better control of the lithium diffusion techniques and the fabrication parameters.

Table 5.

SUMMARY OF I-V CHARACTERISTICS OF JPL SHIPMENT GROUPS

OUP	SILICON	RESIST.	LITHIUM			Cell 28 C, AMO, 140 mW/cm^2			CPF	Co	N_d	No.
			TEMP.	TIME	SOURCE	I_{sc}	V_{oc}	P_{max}				
		ohm/cm	°C	min.		mA	mV	mW		nf/cm^2	cm^{-3}	Cells
-13A	OR	30	330	180	PO	72.2	604	30.5	.695	6.4	$4.5X10^{14}$	30
-13B	OR	30	330	420	PO	70.7	596	30.0	.705	6.2	$4.0X10^{14}$	30
-13C	OR	30	340	180	PO	70.6	609	31.0	.715	6.9	$5.0X10^{14}$	30
-13D	OR	30	340	420	PO	71.3	598	30.5	.715	5.7	$3.5X10^{14}$	30
-13E	OR	30	350	300	PO	67.4	604	29.5	.720	7.7	$6.5X10^{14}$	30
-13F	OR	30	350	300	PO	70.3	602	30.2	.710	7.6	$6.5X10^{14}$	30
-13G	OR	30	360	180	PO	69.6	611	31.0	.725	7.8	$6.5X10^{14}$	30
-13H	OR	30	360	420	PO	71.0	594	30.5	.725	5.8	$3.5X10^{14}$	30
-13I	OR	30	370	240	PO	66.0	604	29.0	.725	7.6	$6.5X10^{14}$	30
-13J	OR	30	370	360	PO	66.6	597	29.0	.730	6.5	$4.5X10^{14}$	30
-14A	OL	15	375	180	PO	61.1	587	26.8	.745	10.7	$1.3X10^{15}$	30
-14B	OR	30	375	180	PO	64.4	603	29.0	.745	9.2	$9.5X10^{14}$	30
-14C	OL	15	350	300	PO	63.9	581	27.5	.735	9.4	$9.5X10^{14}$	30
-14D	OR	30	350	300	PO	67.0	598	29.5	.735	7.6	$6.5X10^{14}$	30
-15A	OL	15	350	240	PO	66.3	589	28.3	.725	10.0	$1.2X10^{15}$	30
-15B	OL	15	350	240	EV	64.8	589	28.3	.740	9.4	10^{15}	30
-15C	OL	75	350	240	PO	65.0	588	28.7	.750	9.2	$9.5X10^{14}$	30
-15D	OL	75	350	240	EV	61.9	595	27.5	.745	9.3	$9.5X10^{14}$	30
-15E	OR	30	350	240	PO	67.3	605	30.0	.735	8.0	$7X10^{14}$	30
-15F	OR	30	350	240	EV	65.8	606	30.2	.755	8.6	$8X10^{14}$	30
-15G	OR	30	350	480	EV	64.9	607	29.5	.750	8.2	$7.5X10^{14}$	30
-16A	OR	20	370	180	EV	67.5	609	31.0	.750	9.7	10^{15}	180
-16B	OR	20	370	180	EV	67.5	613	31.6	.760	9.6	10^{15}	180
-17	OR	10	370	180	EV	68.7	614	31.7	.750	10.3	$1.3X10^{15}$	120
-18A	OR	20	350	120	EV	68.2	613	32.3	.770	8.9	$9X10^{14}$	60
-18B	OR	20	370	120	EV	64.8	609	30.6	.775	9.2	$9.5X10^{14}$	60
-18C	OR	20	360	120	EV	65.7	606	30.5	.770	9.3	$9.5X10^{14}$	60

When Nd exceeds 6.5 x 10^{14} cm^{-3} for OR silicon and 8.5 x 10^{14} cm^{-3} for OL silicon, the associated concentration gradient exceeds 10^{19} cm^{-4}, a value considered adequate for good recovery after typical fluences.

In order to ensure that all cells in a group show identical recovery performance, the irradiation groups (Ref. 3) have suggested that the lithium concentration gradient ratio within the group should be held to within a two-to-one or three-to-one ratio.

Figure 16 shows fair correlation between the ratio of lithium gradient and the total spread in zero-bias capacitance for several cell groups. Although zero-bias capacitance is probably not the best single evaluation method, the figure shows that it has served a useful purpose in monitoring greater control in lithium diffusion.

Figures 17 through 24 give a histogram plot for the number of cells with various Co values for all shipped groups. The gradual tightening of control is clearly seen, even with increase in the numbers processed.

3.7 More Complex Structures

The present design of lithium cell with suitably chosen silicon and lithium diffusion conditions can give cells with good performance for many possible missions. Any further complexity added to the cell design must be justified by the more severe conditions imposed by particular missions.

The study of two of the possible complexities needed to maintain cell stability following high fluence irradiation has been continued this year.

1. Use of Additional N+ Layer at the Back Surface

This layer, using donors other than lithium, has been used particularly with oxygen-lean silicon to reduce the back contact resistance. However, for unirradiated cells, present contact resistances are satisfactorily low. More tests are needed to check the threshold fluence at which carrier removal by lithium depletion (occurring during the recovery phase following irradiation) increases the contact resistance appreciably.

2. Use of Additional N+ Layer Near the Front Surface

Past results have shown that this layer can increase the stability of the PN junction when lithium carriers are removed following high fluences. Again tests are needed to find the threshold fluence which makes this N+ layer necessary. The threshold fluence will be higher as the

starting donor concentration is increased. Thus, comparison of the C-15 Lopex groups will be of interest.

The other possible use of the front surface N+ layer is to control the final distribution of lithium near the PN junction after the lithium diffusion cycle. Tests in progress will show if any advantageous distributions can be obtained.

3. Front Surface Introduction of Lithium

In the past year, tests continued on the possible merits of introducing lithium through the front surface of both P/N and N/P cells. The cells made to date with this method did not show any advantages over the conventional design cells.

3.8 Other Topics

3.8.1 Contact Materials

As seen above, titanium-silver contacts can allow CPF values as high as 0.77 to be obtained, with good adhesion. Aluminum contacts have also been used, and with close control, can also reach the same high CPF values.

3.8.2 Contact Sintering Cycles

Good adhesion was obtained using sintering cycles with temperatures and times below those used for lithium diffusion. Care was taken in setting up these sinter cycles to ensure that there was no measurable change in lithium concentration during sintering, or any inherent contact resistance increase. The best cycles were 10 minutes at temperatures around 400°C.

Some tests were made of sintering cycles using temperatures in excess of lithium diffusion temperatures, to determine threshold for changes.

Table 6 shows the changes observed in I_{sc}, V_{oc} and capacitance for typical cells from C-14 and C-15, following one sinter-cycle of 600°C - 5 minutes. The OL silicon showed greater changes than OR silicon, as expected from the higher mobility of lithium. In general, I_{sc} increased (mostly in long wavelength response) and capacitance decreased. The observed decrease in capacitance would seriously reduce the recoverability.

Another test used OR silicon and OL silicon, both BCl_3 diffused with 2 minute tack-on, and OL silicon with 8 minute tack-on. All cells were lithium diffused at 400°C - 120 min., using both paint-on and evaporated sources. The cells were measured and then given a series of sinter-cycles (600°C - 5 min.) and the changes followed. No consistent differences caused by the two lithium source

Table 6.

CHANGES OBSERVED AFTER HIGH TEMPERATURE SINTER CYCLE

OUP	SILICON	RESIST.	LITHIUM TEMP.	LITHIUM TIME	LITHIUM SOURCE	I_{sc}	I_{sc}'	V_{oc}	V_{oc}'	C	C '
		ohm/cm	°C	min.		mA	mA	mV	mV	nF	nF
-14A	OL	15	375	180	PO	57.0	61.0	590	590	28.5	21.0
						57.5	60.5	590	590	27.5	20.0
-14B	OR	30	375	180	PO	60.0	59.5	590	580	16.8	16.0
						59.5	59.5	595	585	18.8	16.7
-14C	OL	15	350	300	PO	64.5	67.0	590	550	17.6	14.6
						61.5	65.5	590	580	29.5	19.6
-14D	OR	30	350	300	PO	62.5	66.0	605	600	18.0	15.2
						64.5	66.5	610	585	12.8	11.2
-15A	OL	15	350	240	PO	62.0	65.0	585	580	22.5	16.0
						64.5	68.0	585	565	23.0	15.6
-15B	OL	15	350	240	EV	60.0	63.5	585	585	24.5	18.4
						60.5	63.5	590	585	25.5	19.2
-15C	OL	75	350	240	PO	65.5	69.0	590	570	21.0	13.0
						66.5	69.0	600	585	22.0	14.6
-15D	OL	75	350	240	EV	64.5	70.0	580	580	14.0	10.3
						63.0	67.0	580	580	17.0	12.3
-15E	OR	30	350	240	PO	66.5	68.5	595	600	16.0	15.8
						68.0	68.0	615	610	16.3	15.9
-15F	OR	30	350	240	EV	69.0	72.0	590	585	13.0	10.8
						71.5	71.5	590	505	9.8	9.2
-15G	OR	30	350	480	EV	65.5	68.0	615	605	15.5	13.6
						65.5	67.0	615	605	15.8	14.0

NOTE: The values with a dash (') were measured after sintering.

conditions were observed. Therefore the spread of values are given in Figures 25 through 27. Table 7 shows the calculated loss in lithium atoms near the PN junctions during the sinter series.

3.8.3 Comments

It can be seen that sintering may lead to large changes, some increase in I_{sc}, but often accompanied by serious decrease in lithium near the junction. If sintering relieves some stresses in the silicon, tests should be performed to determine if the stress relief can be provided at the pertinent process step. Any sinter-cycle used should be evaluated, measuring the changes in all I-V characteristics and particularly by monitoring the lithium concentration.

4.0 Conclusions

This phase of the research program has consolidated the use of single-cycle, moderate lithium diffusion schedules. With tighter control of the fabrication steps, cells with good output and containing adequate and well controlled lithium concentrations were obtained in reasonably large numbers. The analytical methods used proved adequate to guide the work to the present stage and appear generally applicable to further scale-up. The work has led to lithium-doped cells which have several possible applications in space missions. In addition, increased understanding of solar cells in general has resulted from this program.

5.0 Recommendations

The above results show that there is motive for scale-up of the lithium cell fabrication. The present techniques are inherently capable of direct scaling, but the important steps of boron and lithium diffusion need re-evaluation to qualify as proven production steps.

6.0 References

1. "Research, Development and Fabrication of Lithium Solar Cells", Final Report, Part I, JPL Contract No. 952546, November 23, 1970. (Centralab Semiconductor Division)

2. "Development and Fabrication of Lithium-Doped Solar Cells", P. A. Iles, Proceedings of Fourth Annual Conference on Effects of Lithium Doping on Silicon Solar Cells, JPL, Pasadena, 1971.

Table 7.

FRACTIONAL LOSS IN LITHIUM DURING SINTER CYCLE

All Cells Diffused at 400°C - 120 min.

	No. of cycles (600°C 5 min.)	Fraction of Li Remaining
OL Silicon, 2 min. tack on	0	1.0
	1	0.8
	2	0.45
OL Silicon, 8 min. tack on	0	1.0
	1	0.65
	2	0.30
OR Silicon, 2 min. tack on	0	1.0
	1	0.85
	2	0.85
	3	0.60
	4	0.25

3. "Study to Determine and Improve Design for Lithium-Doped Solar Cells", Final Report JPL Contract 952555, 3 December 1971. (RCA)

4. "Study and Determination of an Optimum Design for Space Utilized Lithium Doped Solar Cells", Final Report, Part II, JPL Contract 952554, 15 July 1971. (TRW)

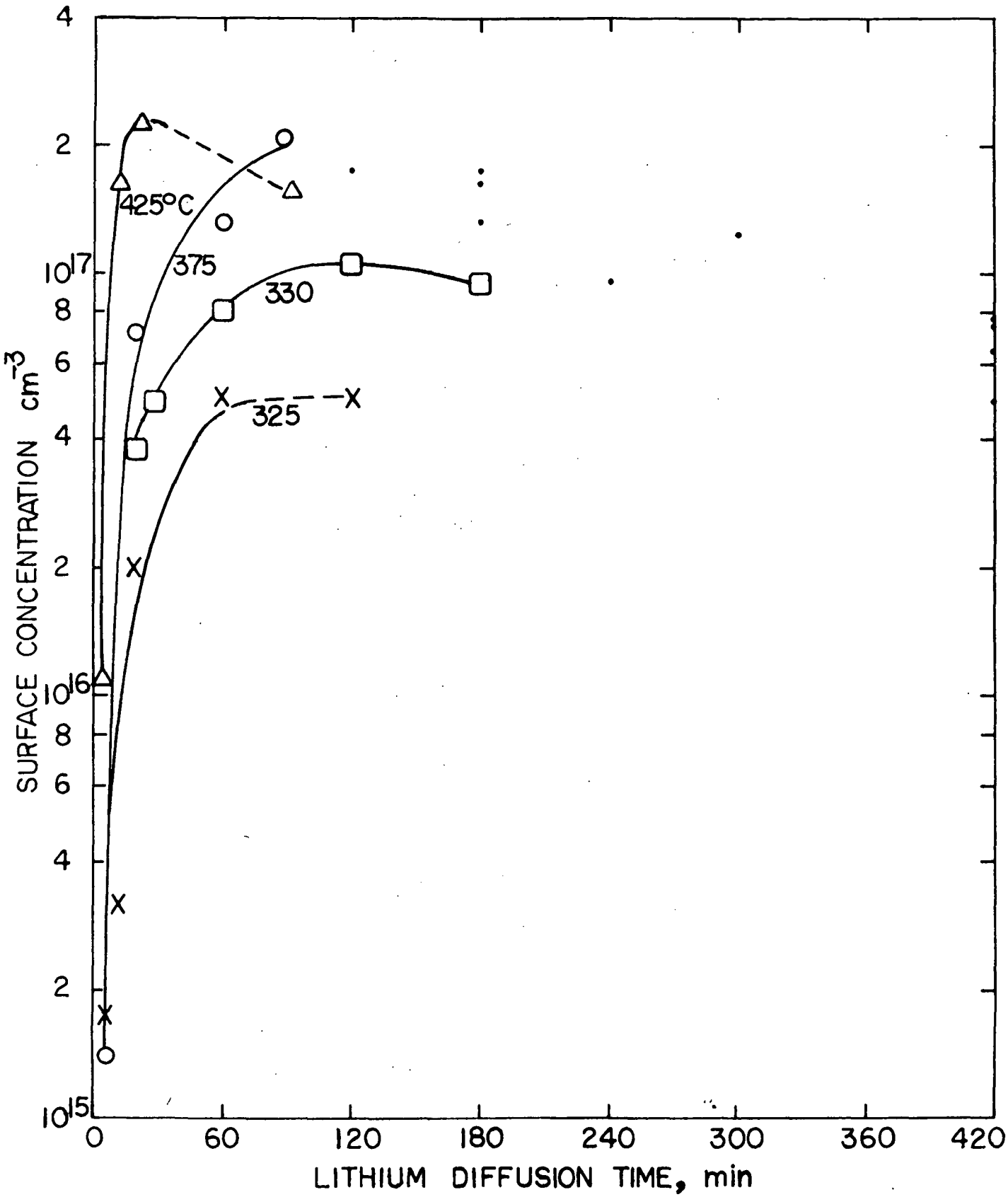

Fig. 1. Build-up of surface concentration of lithium for increasing time at various temperatures

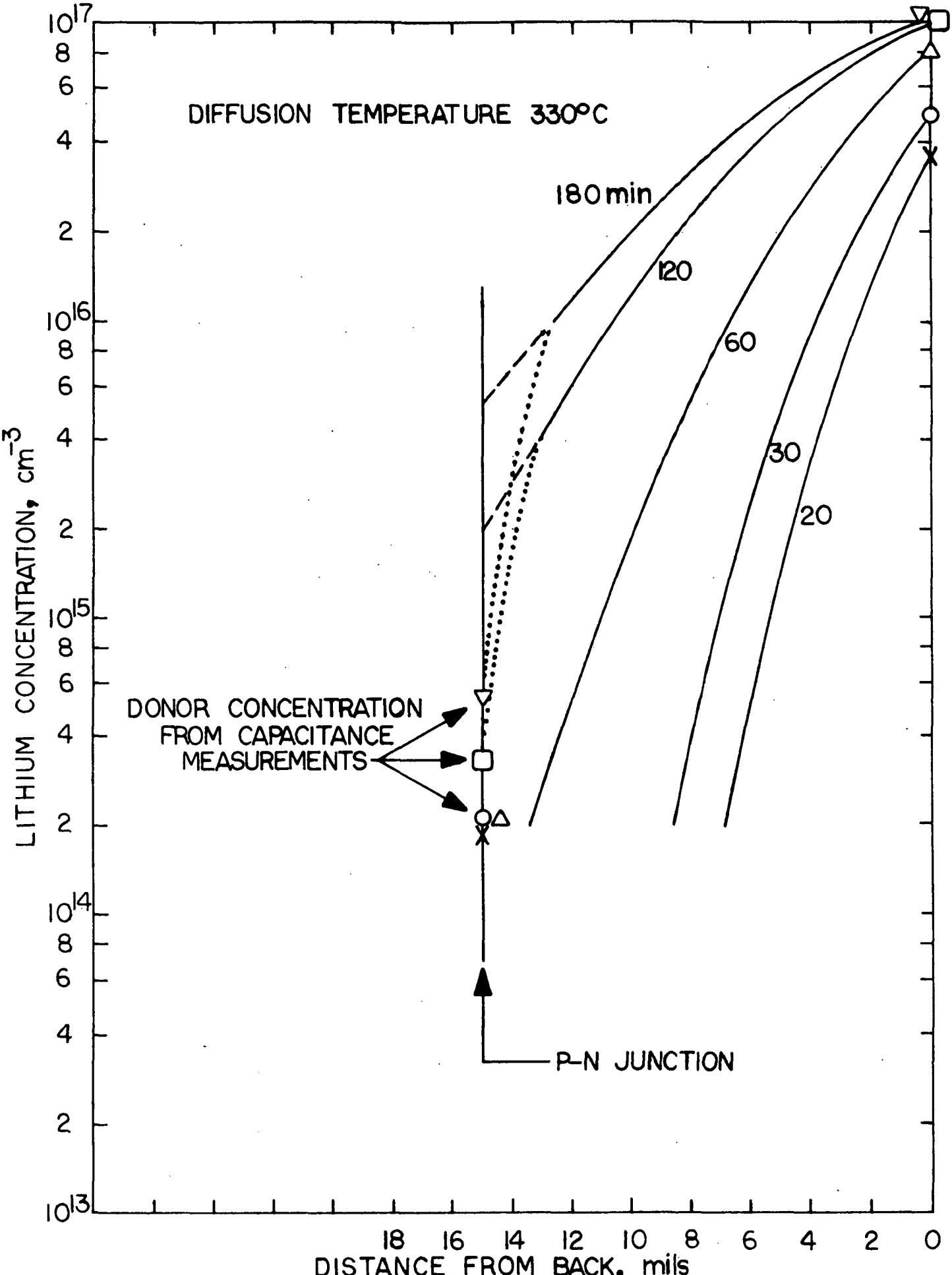

Fig. 2. Changes in lithium concentration profile and the values measured at the P/N junction as the diffusion time at 330°C was increased

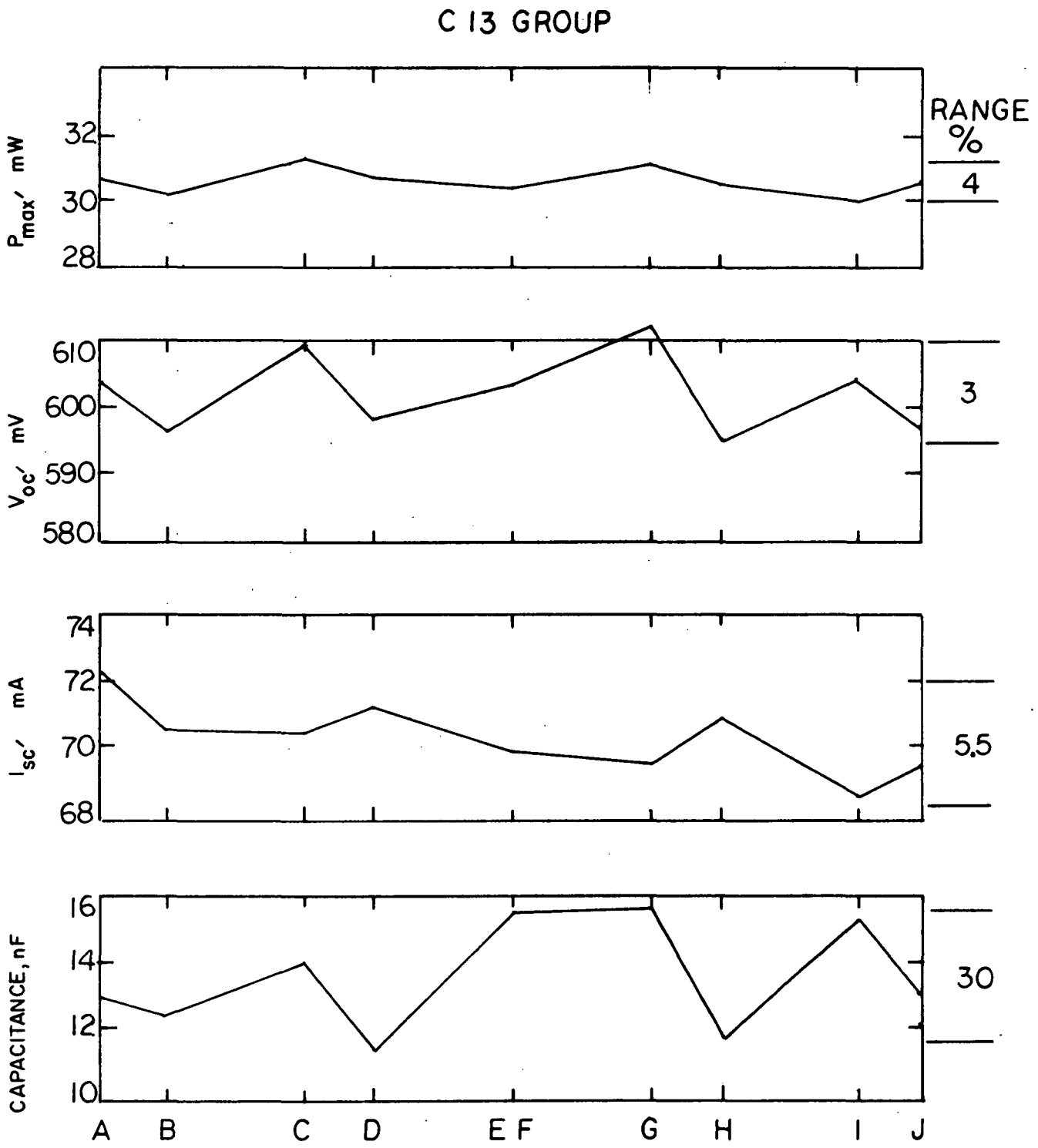

Fig. 3. Average values for P_{max}, V_{oc}, I_{sc}, and capacitance for the ten C13 groups

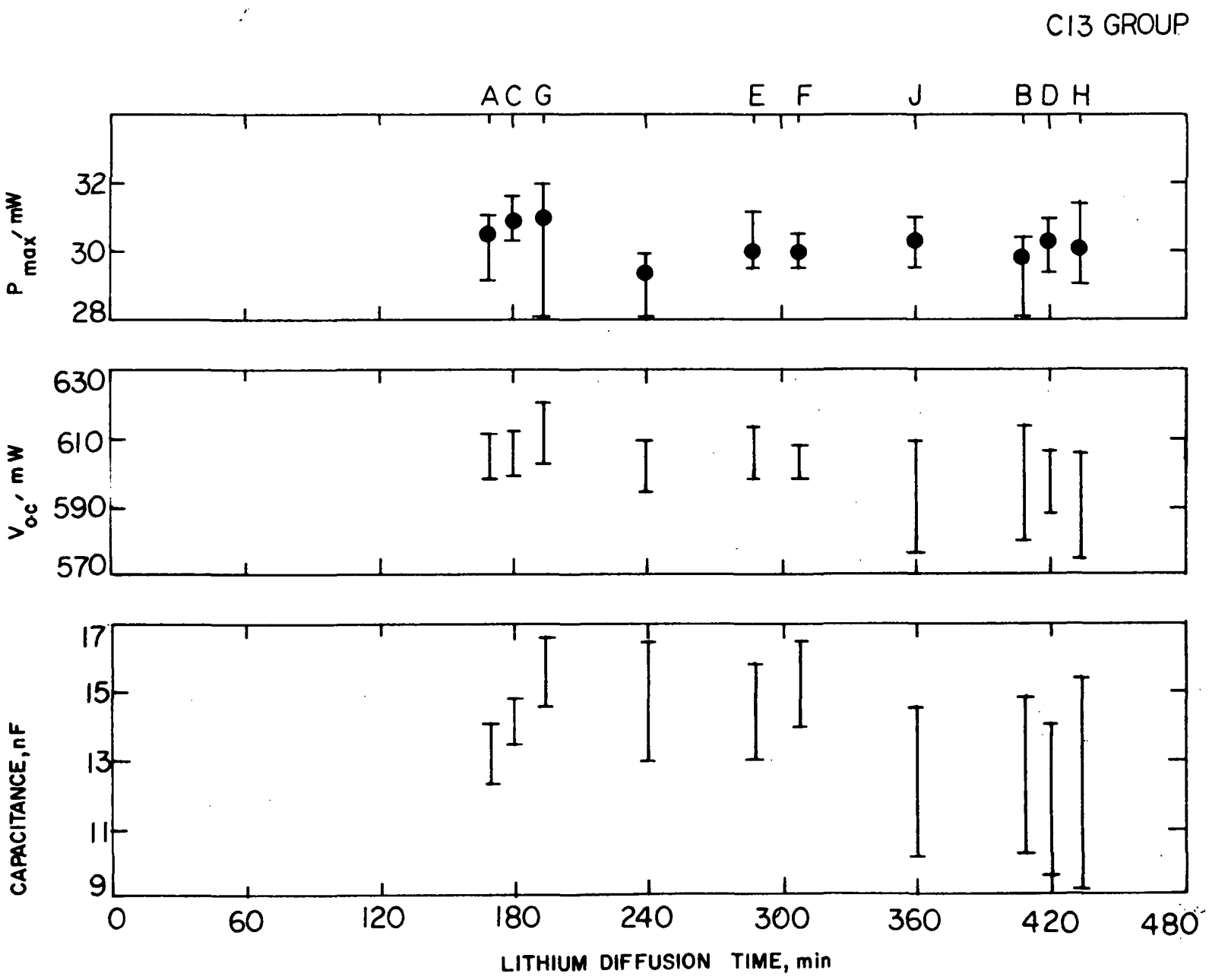

Fig. 4. Average values and spread for P_{max}, V_{oc}, and capacitance for the C13 groups, plotted as a function of diffusion time

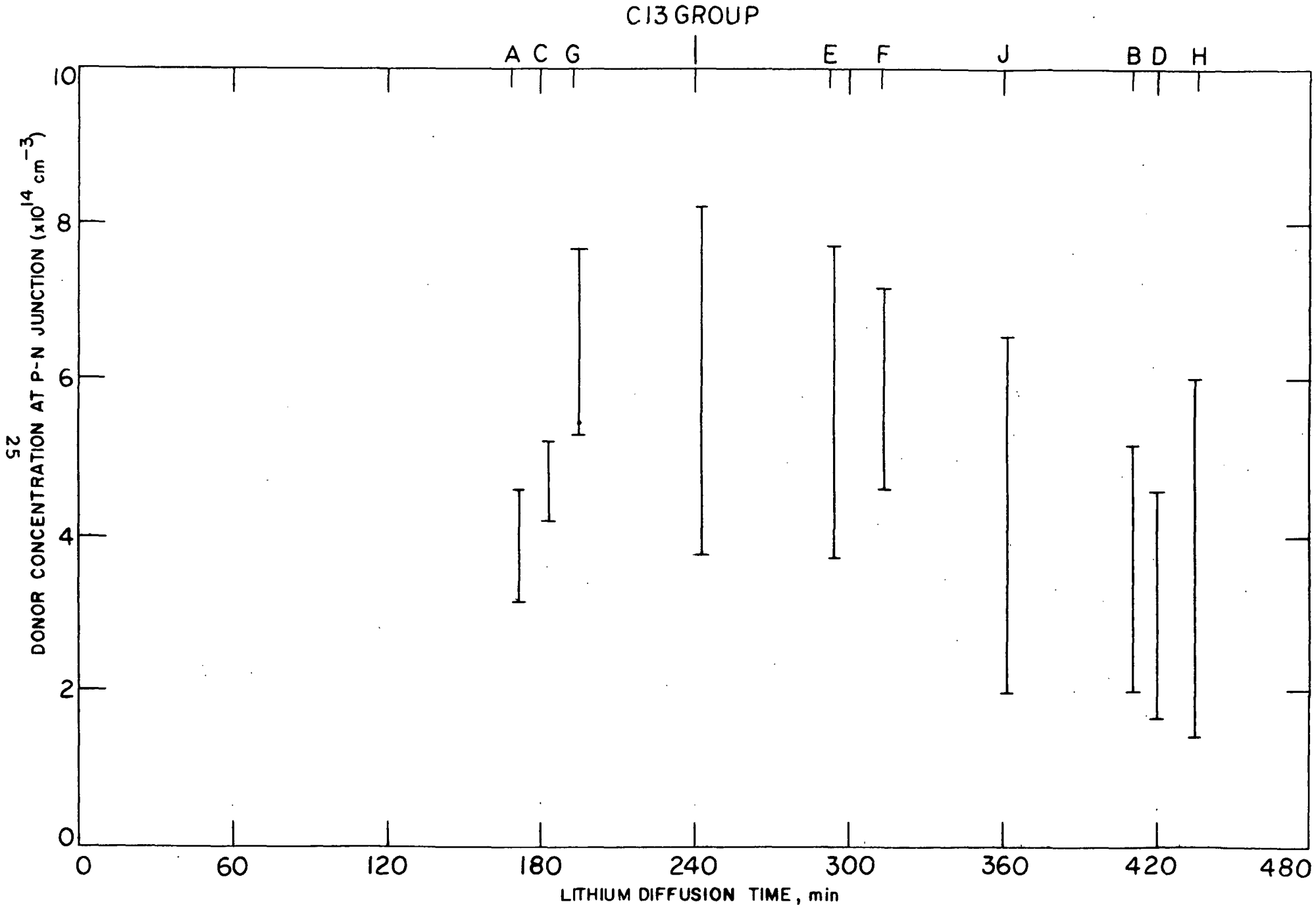

Fig. 5. Average values and spread of donor concentration at the P/N junction, for the ten C13 groups, plotted as a function of diffusion time

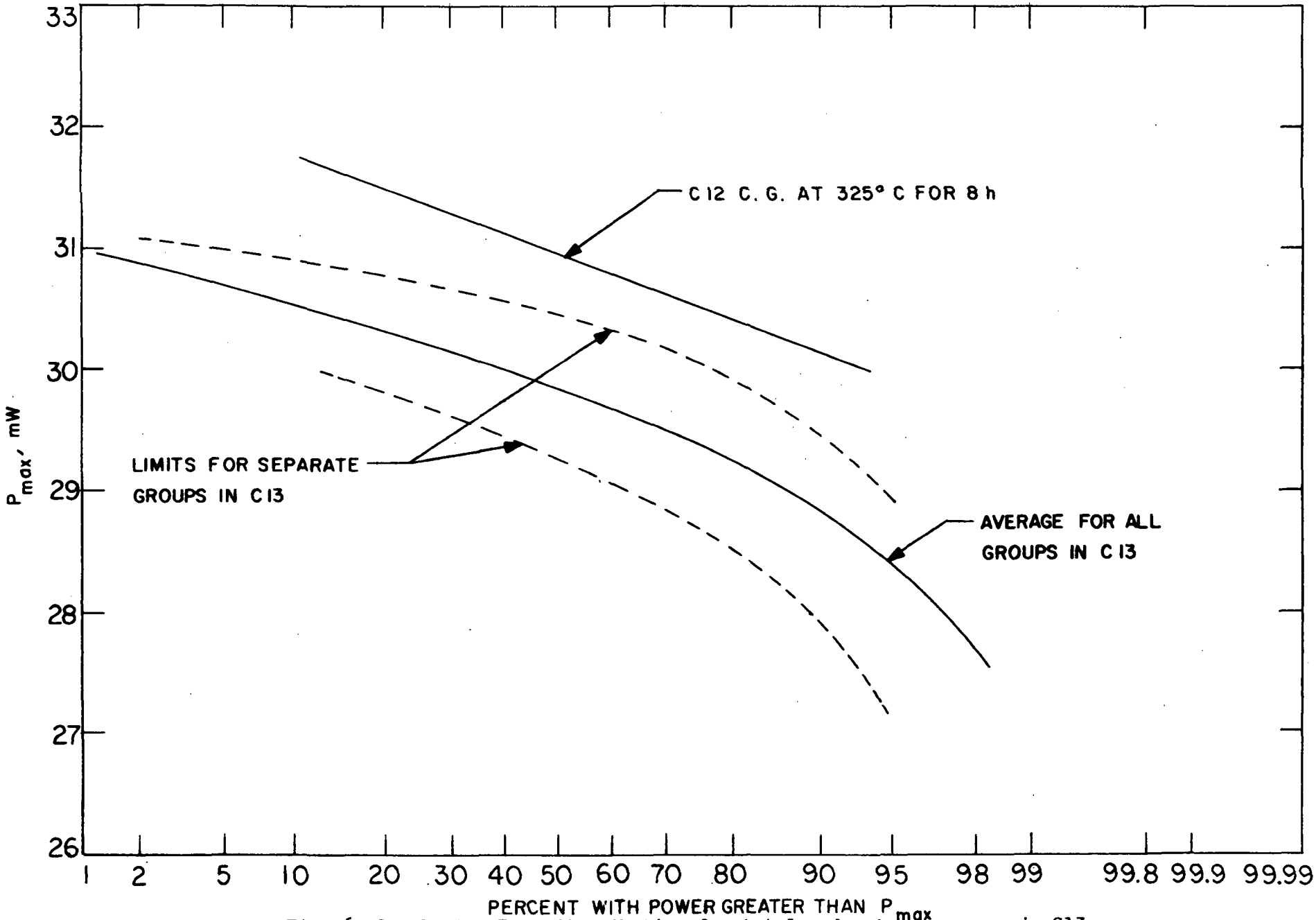

Fig. 6. Cumulative P_{max} distribution for total and extreme groups in C13
(C12 shown for comparison)

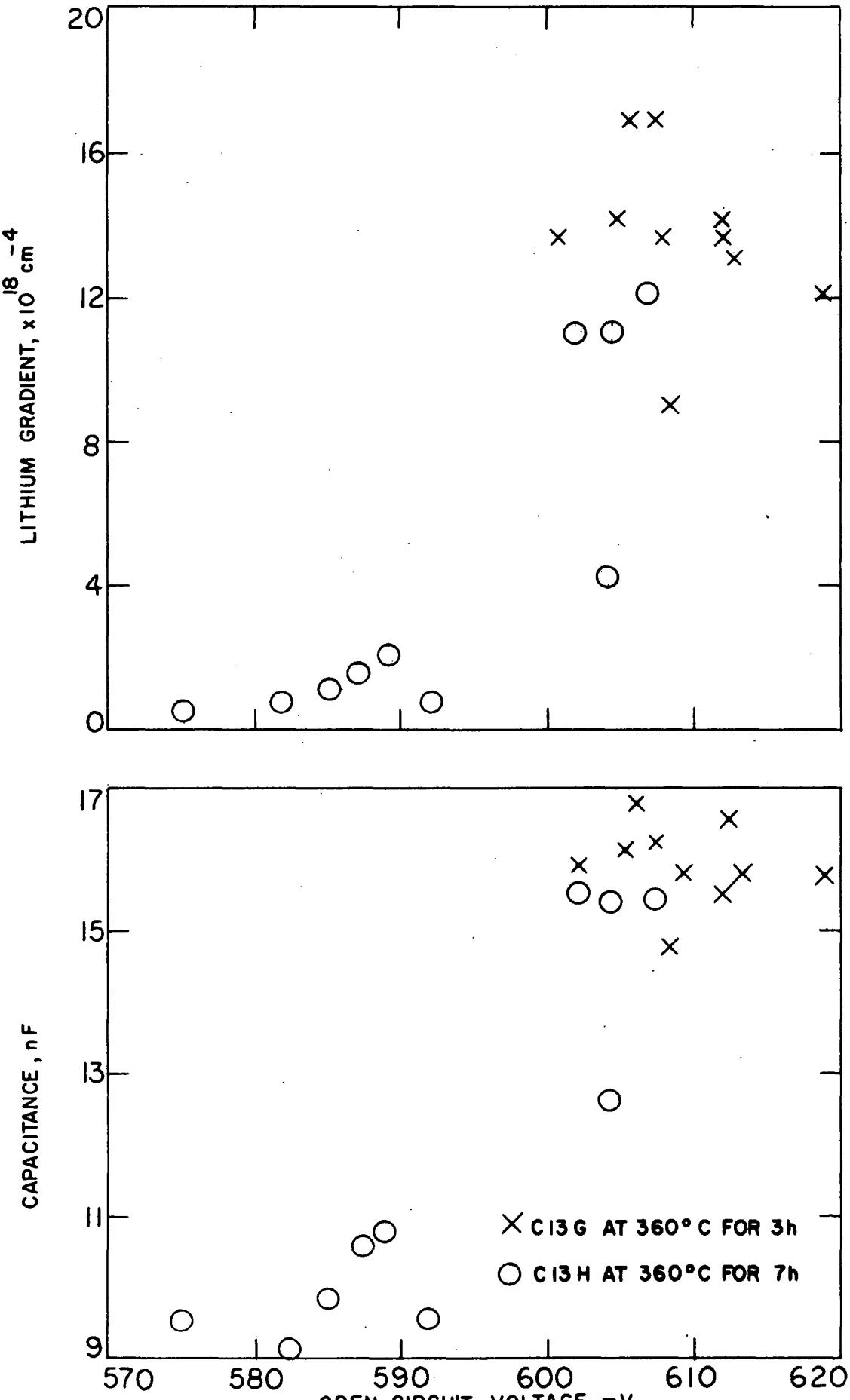

Fig. 7. V_{oc} plotted versus capacitance and lithium concentration gradient near the junction for the two 10-cell groups in C13

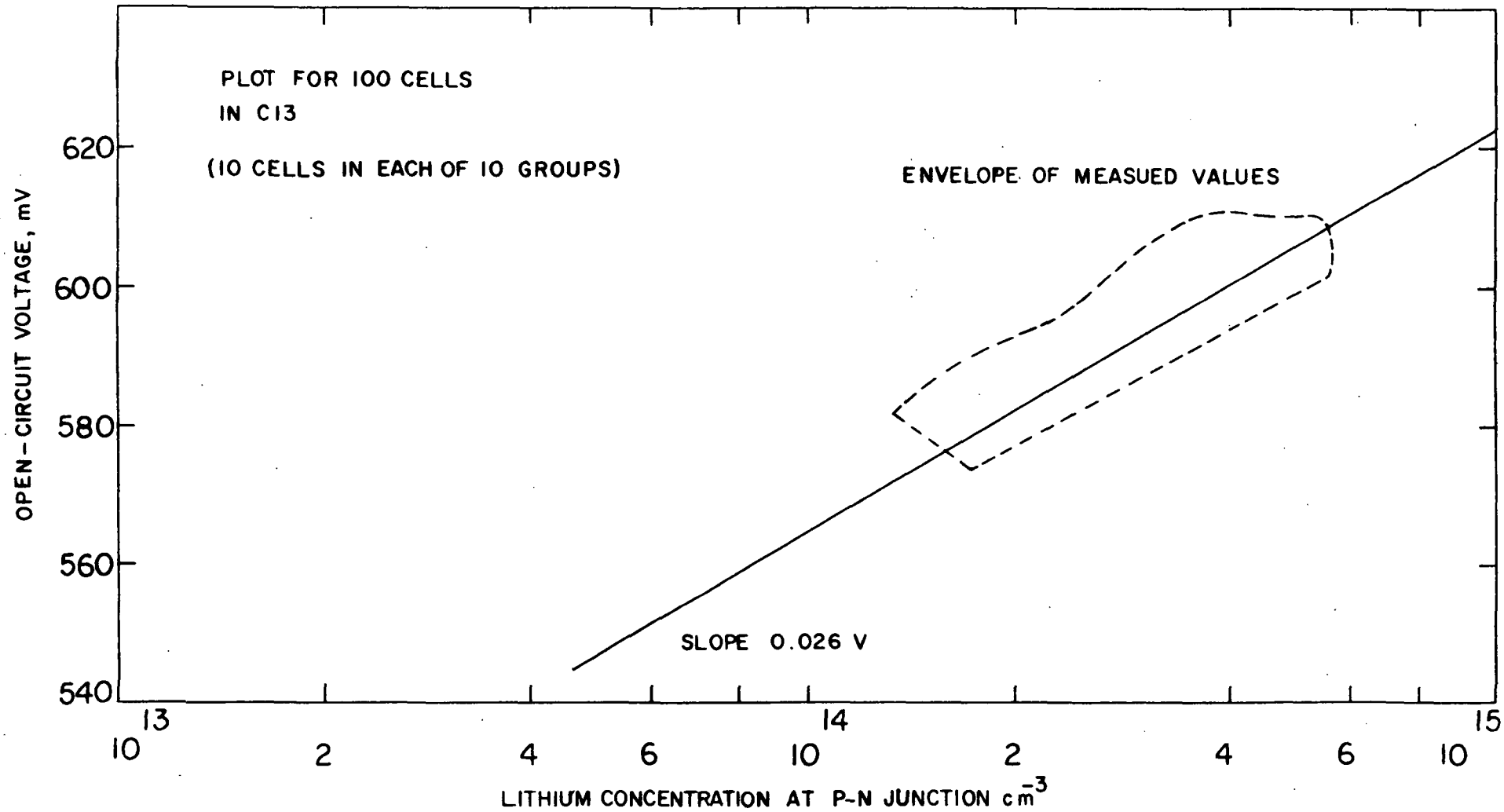

Fig. 8. V_{oc} plotted against logarithm of the donor concentration for 100 cells, 10 in each C13 groups

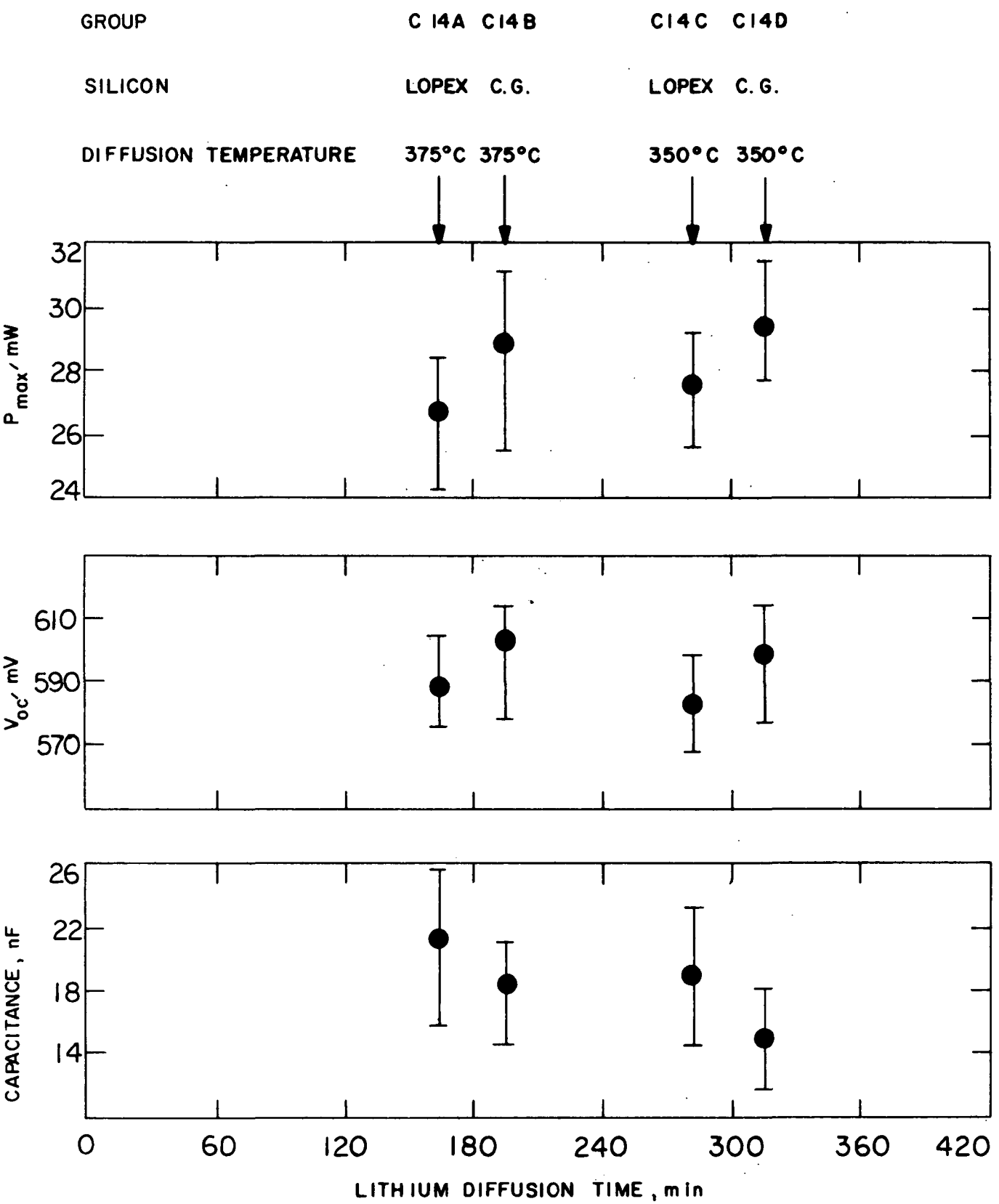

Fig. 9. Average values and spread of P_{max}, V_{oc}, and capacitance for C14 cell groups

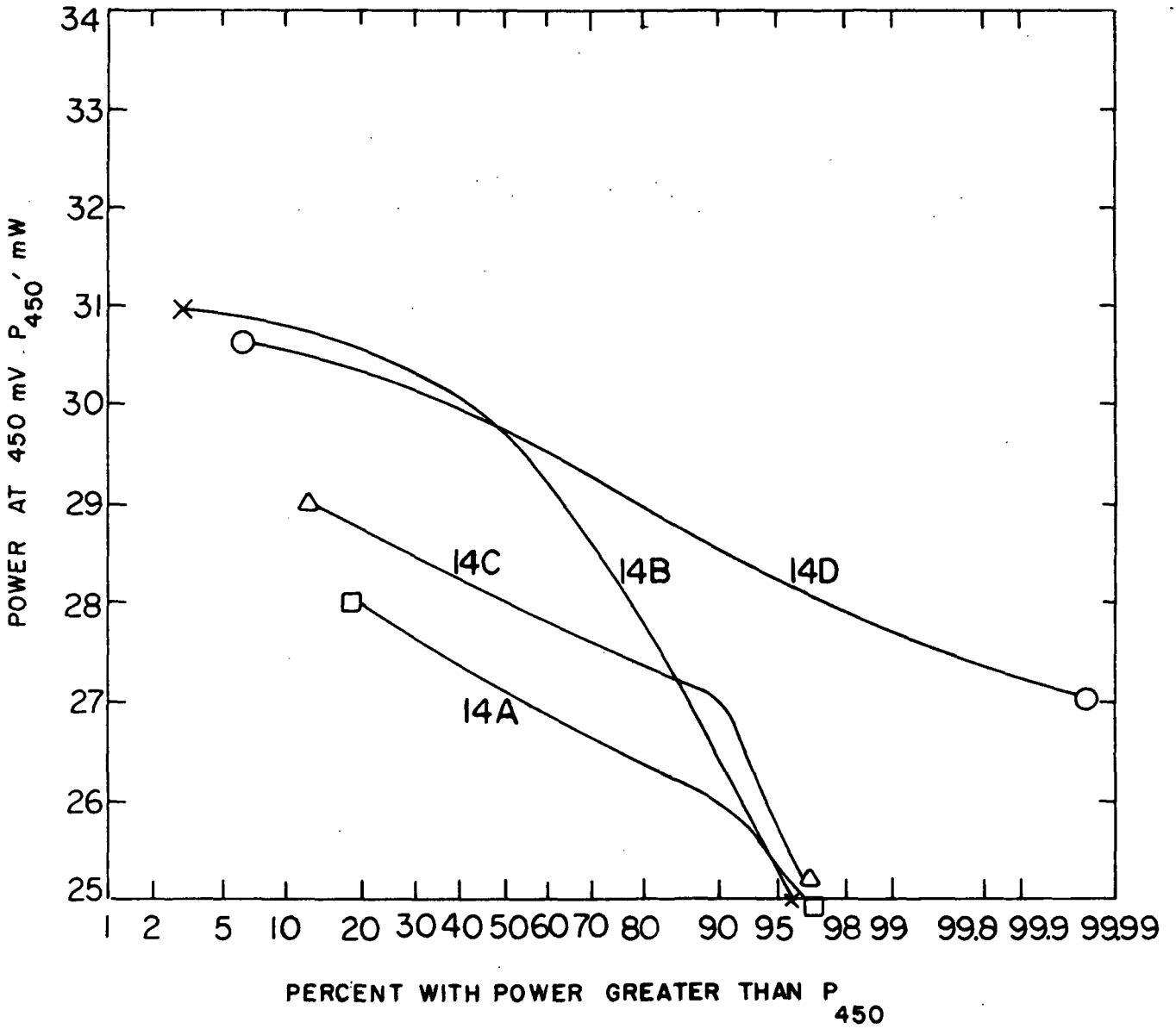

Fig. 10. Cumulative P_{max} plot for JPL shipment C-14

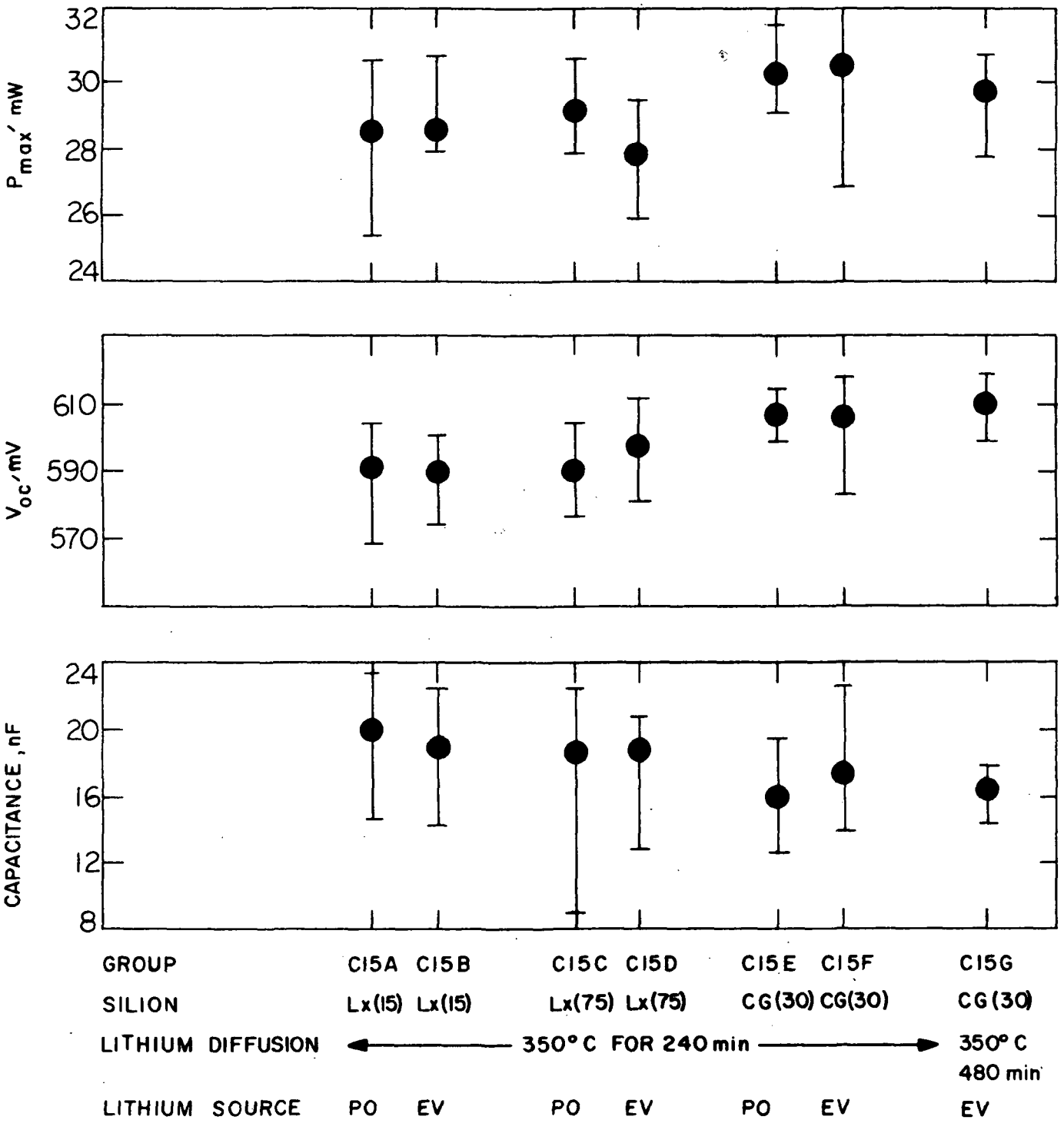

Fig. 11. Average values and spread for P_{max}, V_{oc}, and capacitance for C15 cell groups

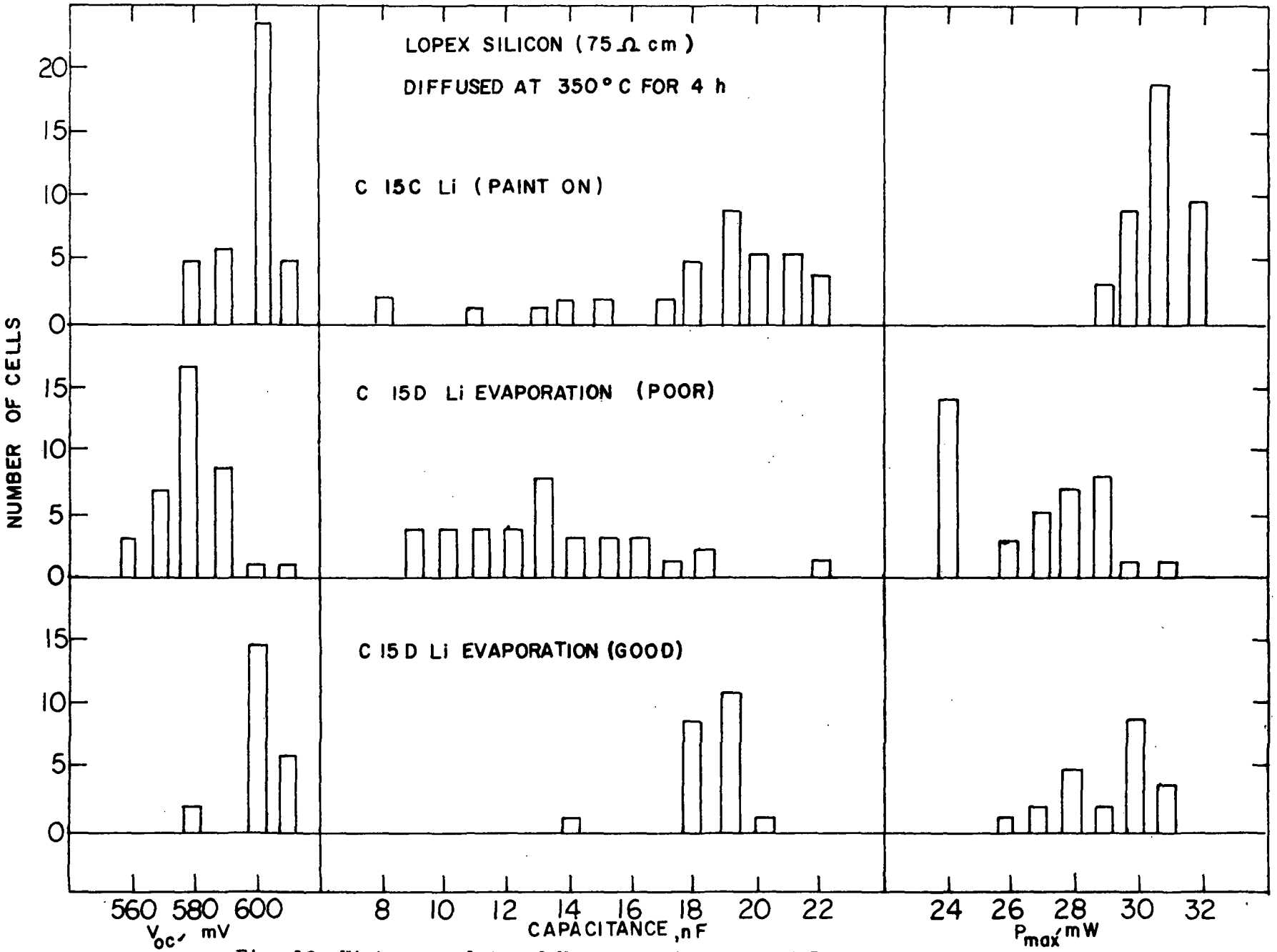

Fig. 12. Histogram plots of V_{oc}, capacitance, and P_{max} for three different conditions of lithium application in two C15 groups

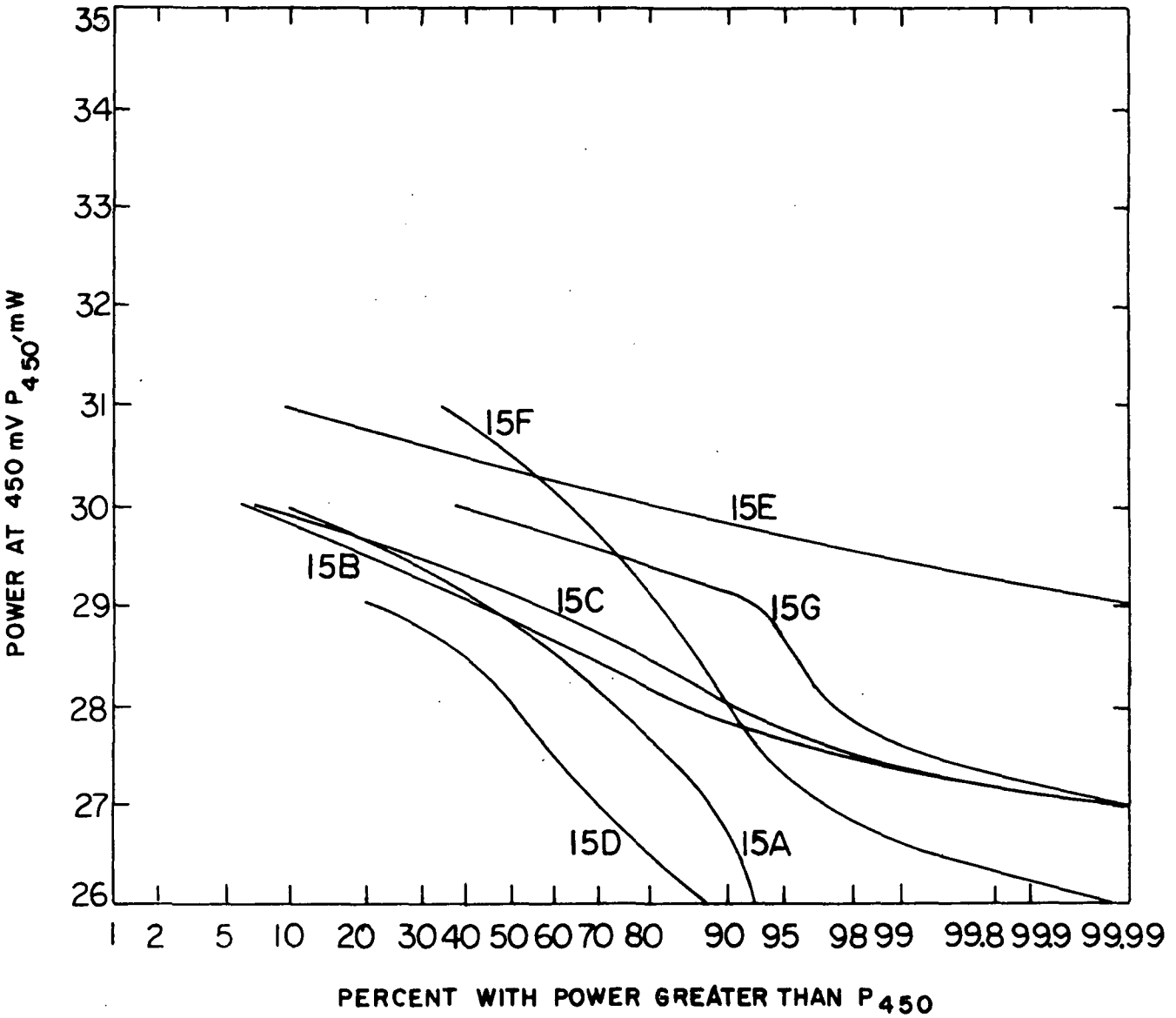

Fig. 13. Cumulative P_{max} plot for JPL shipment C-15

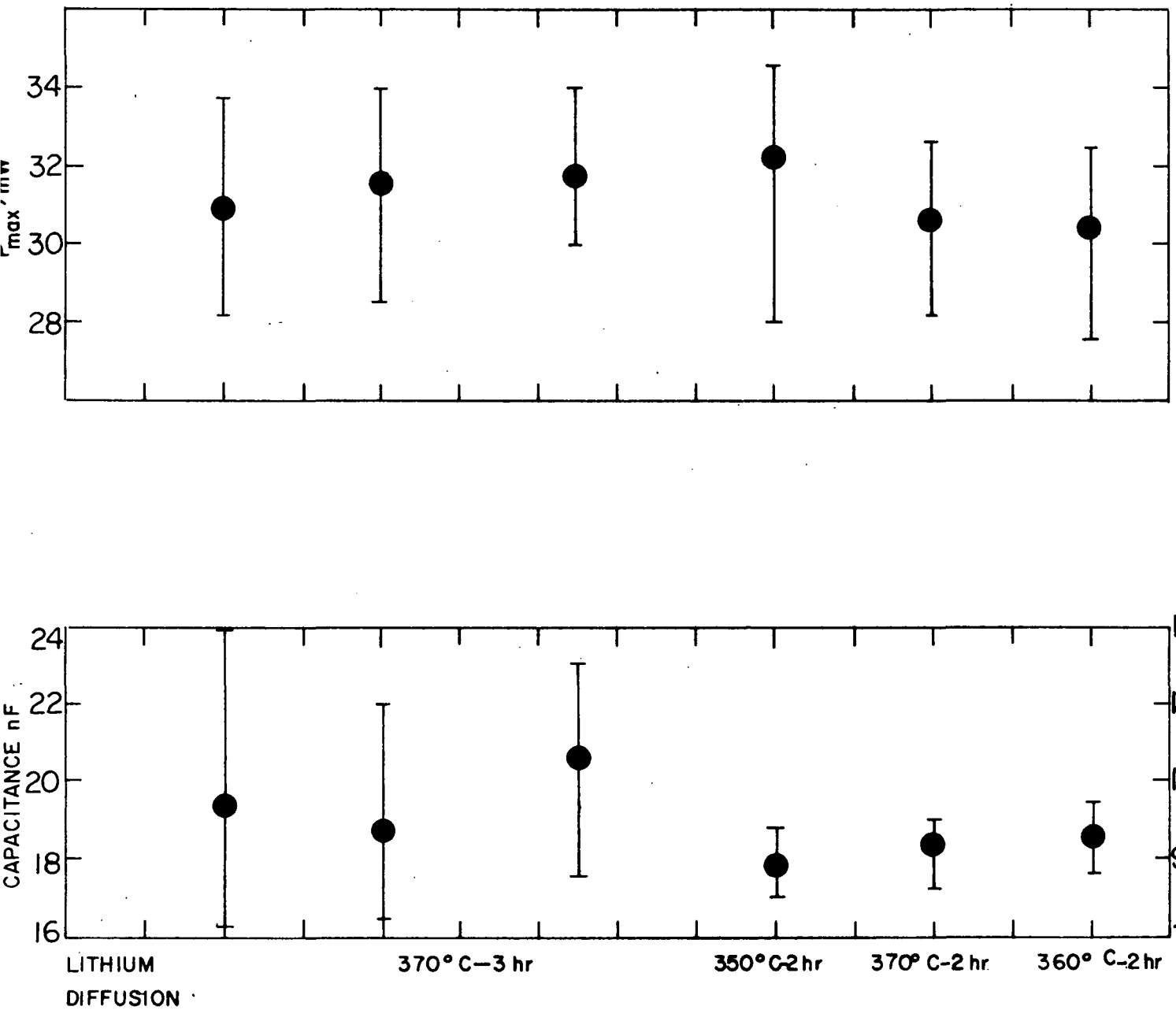

Fig. 14. Maximum power, zero-bias capacitance and donor concentration for six groups of lithium-doped cells

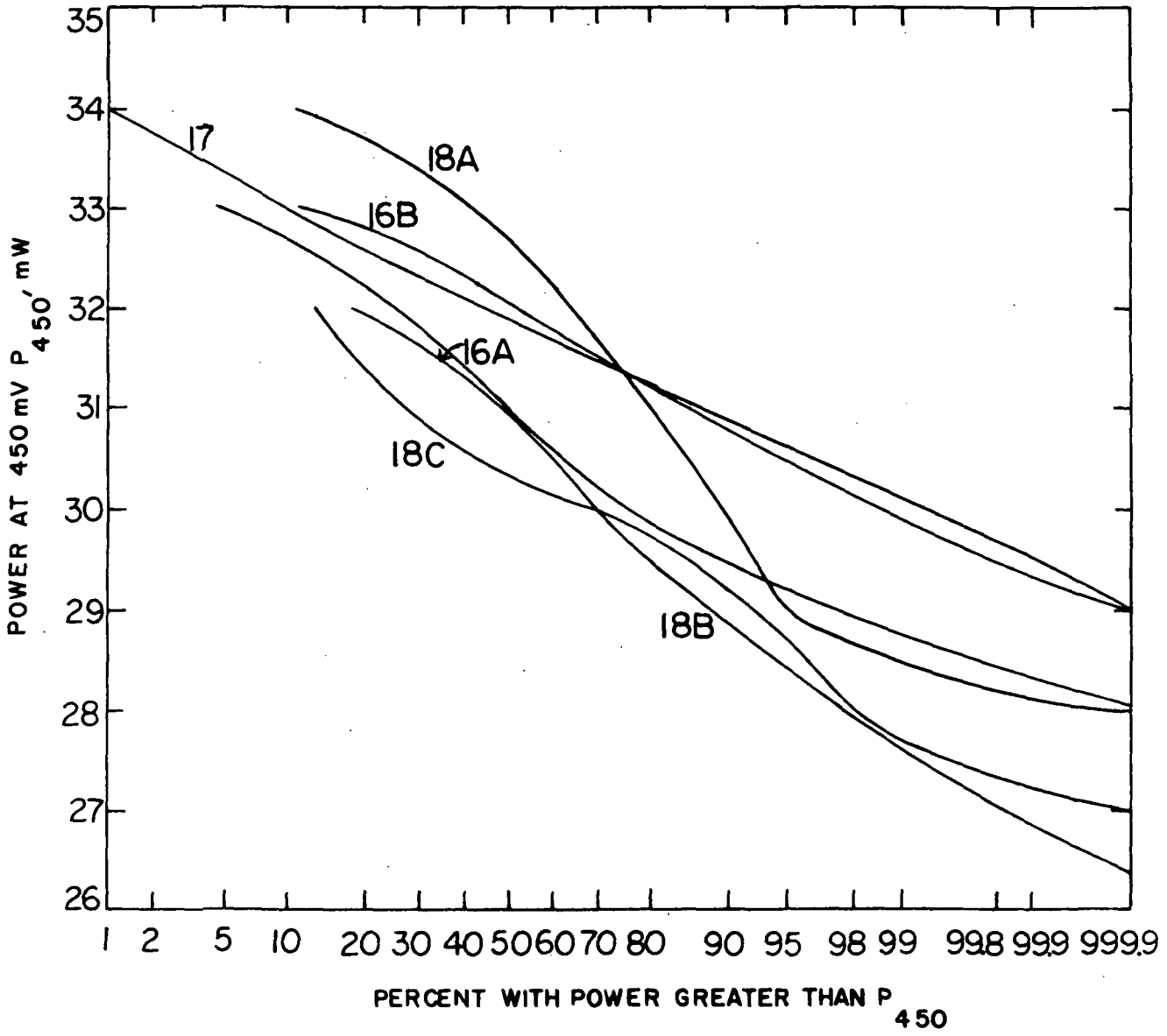

Fig. 15. Cumulative P_{max} plots for JPL shipments C-16, C-17, C-18

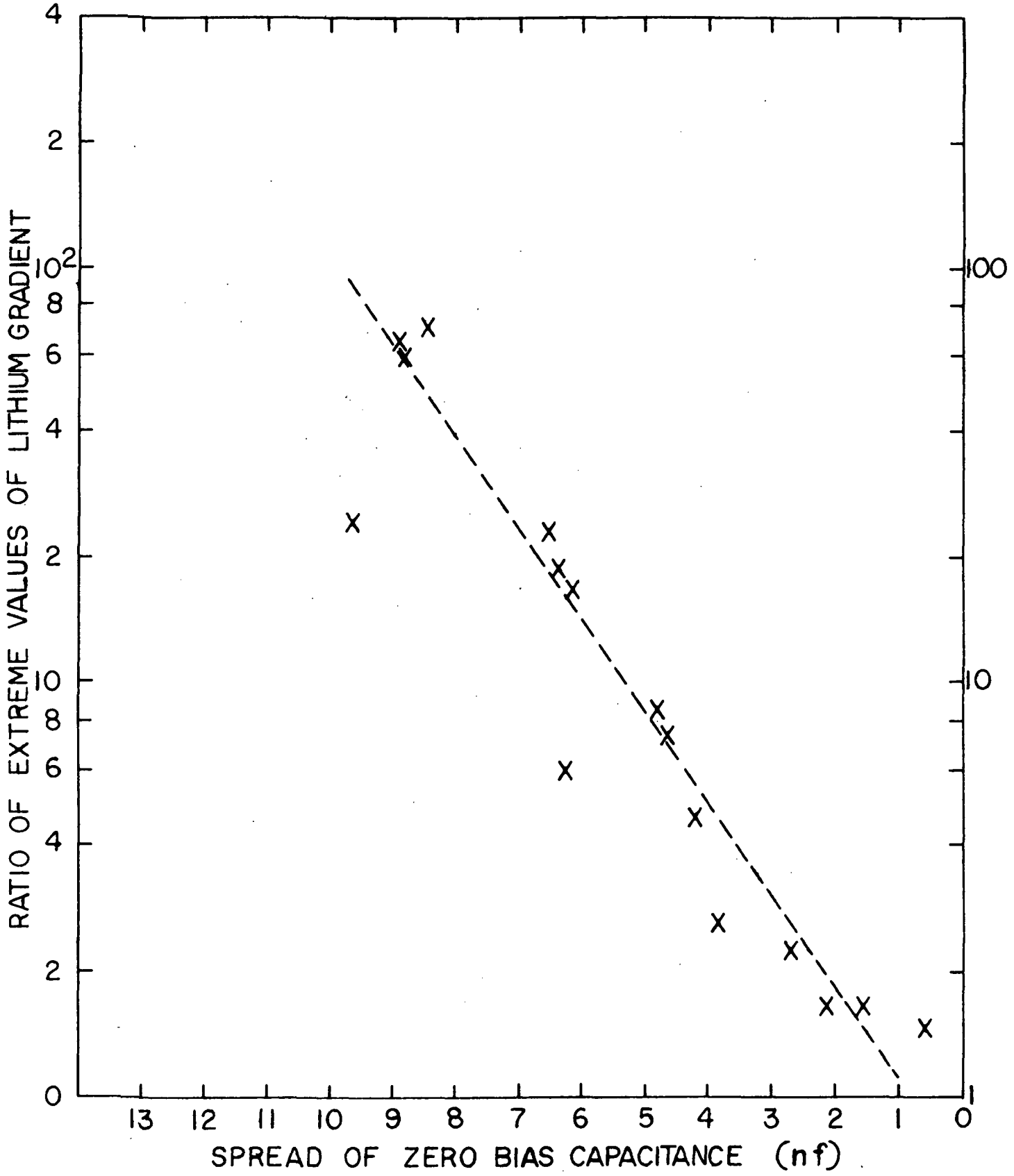

Fig. 16. Comparison of the ratio of the extreme values of lithium gradient and the spread in zero-bias capacitance, for sixteen groups of cells

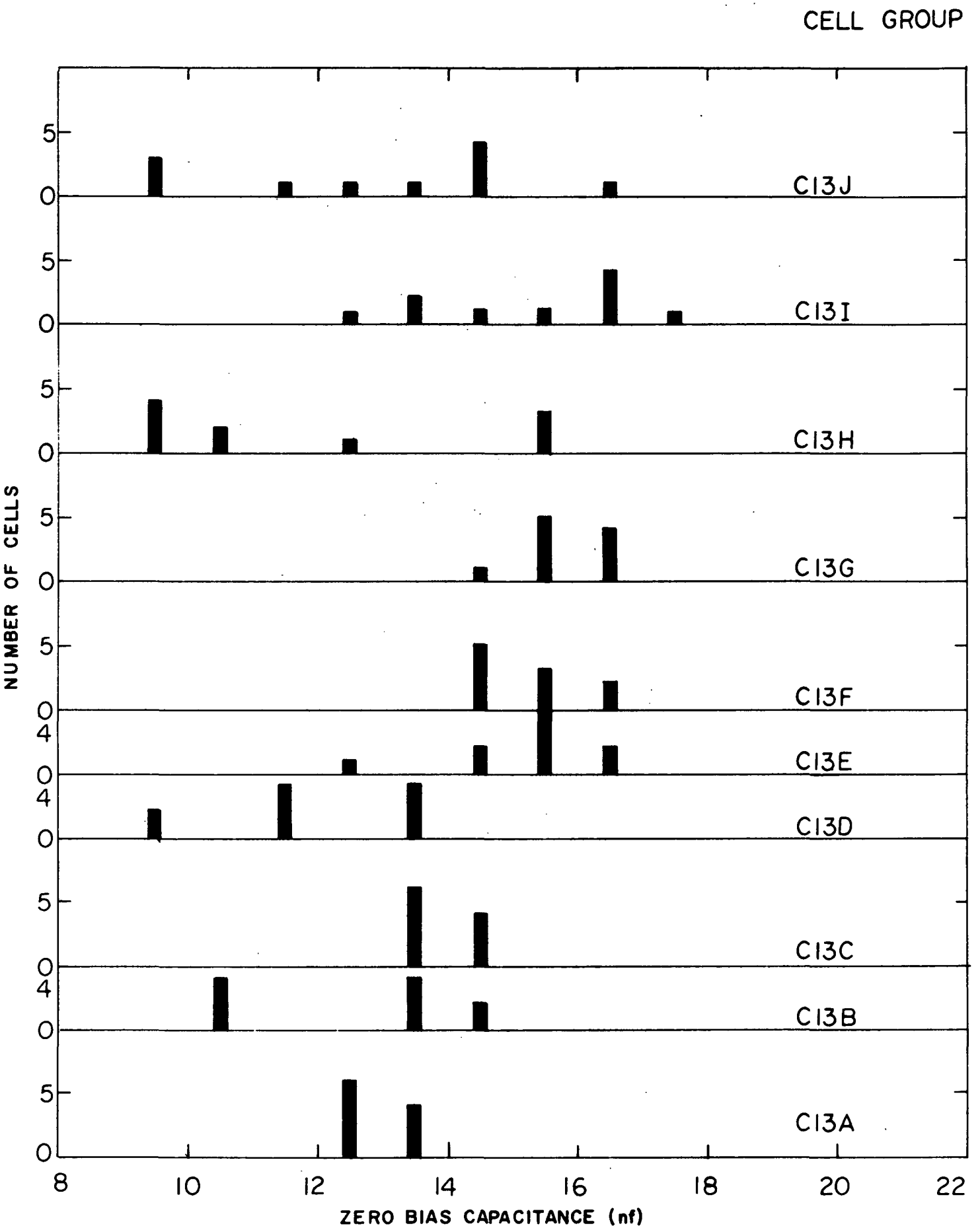

Fig. 17. Capacitance distribution for C-13

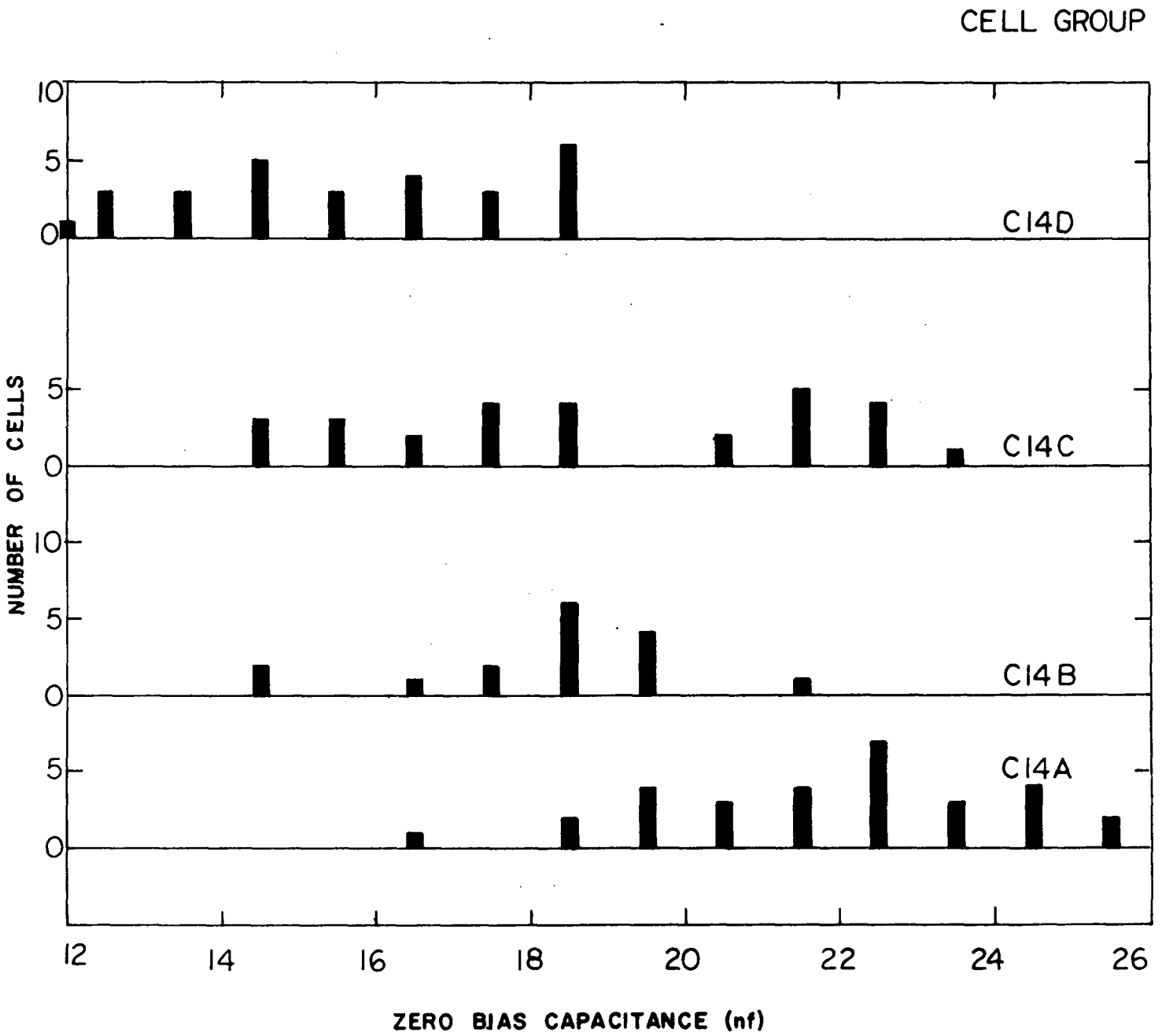

Fig. 18. Capacitance distribution for C-14

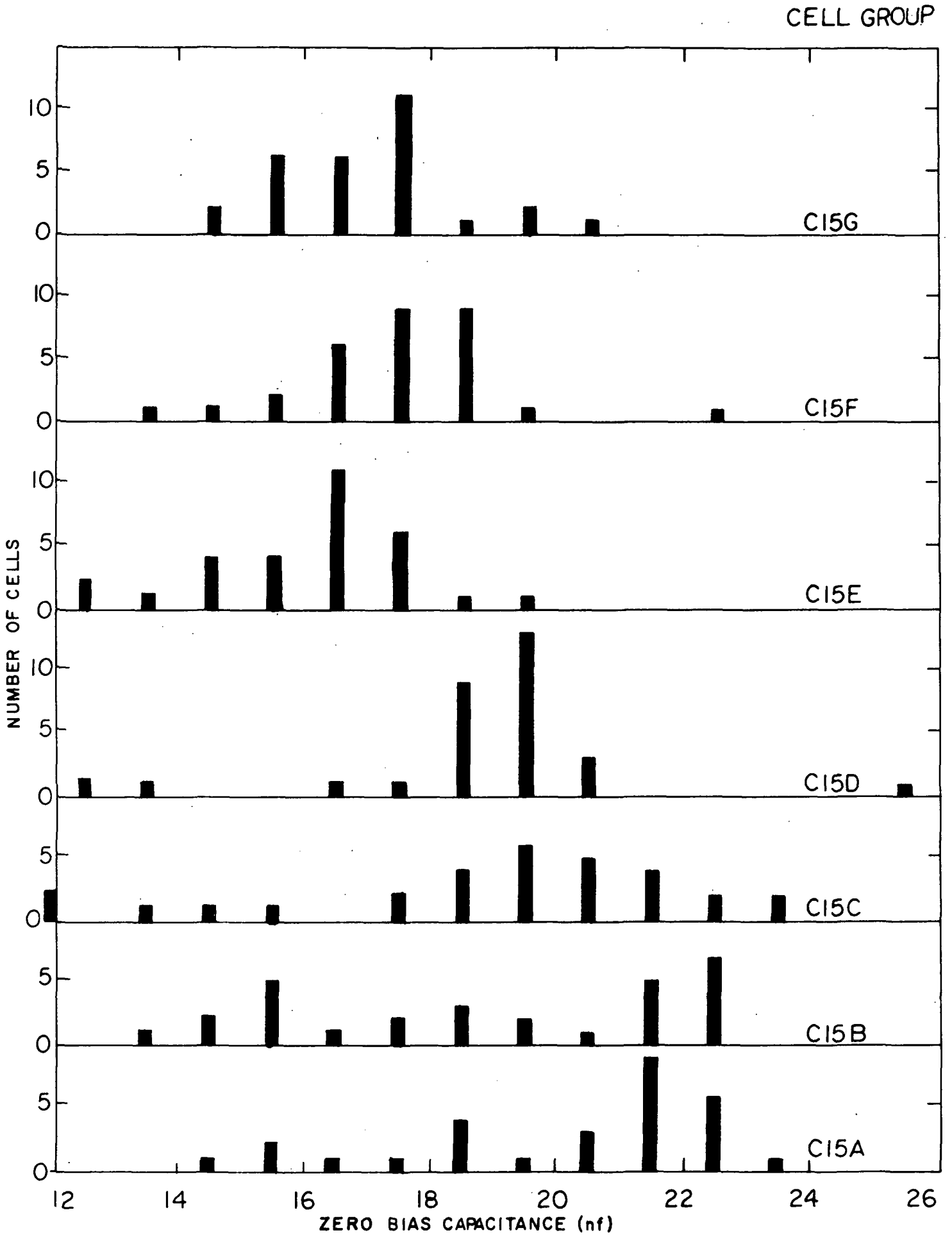

Fig. 19. Capacitance distribution for C-15

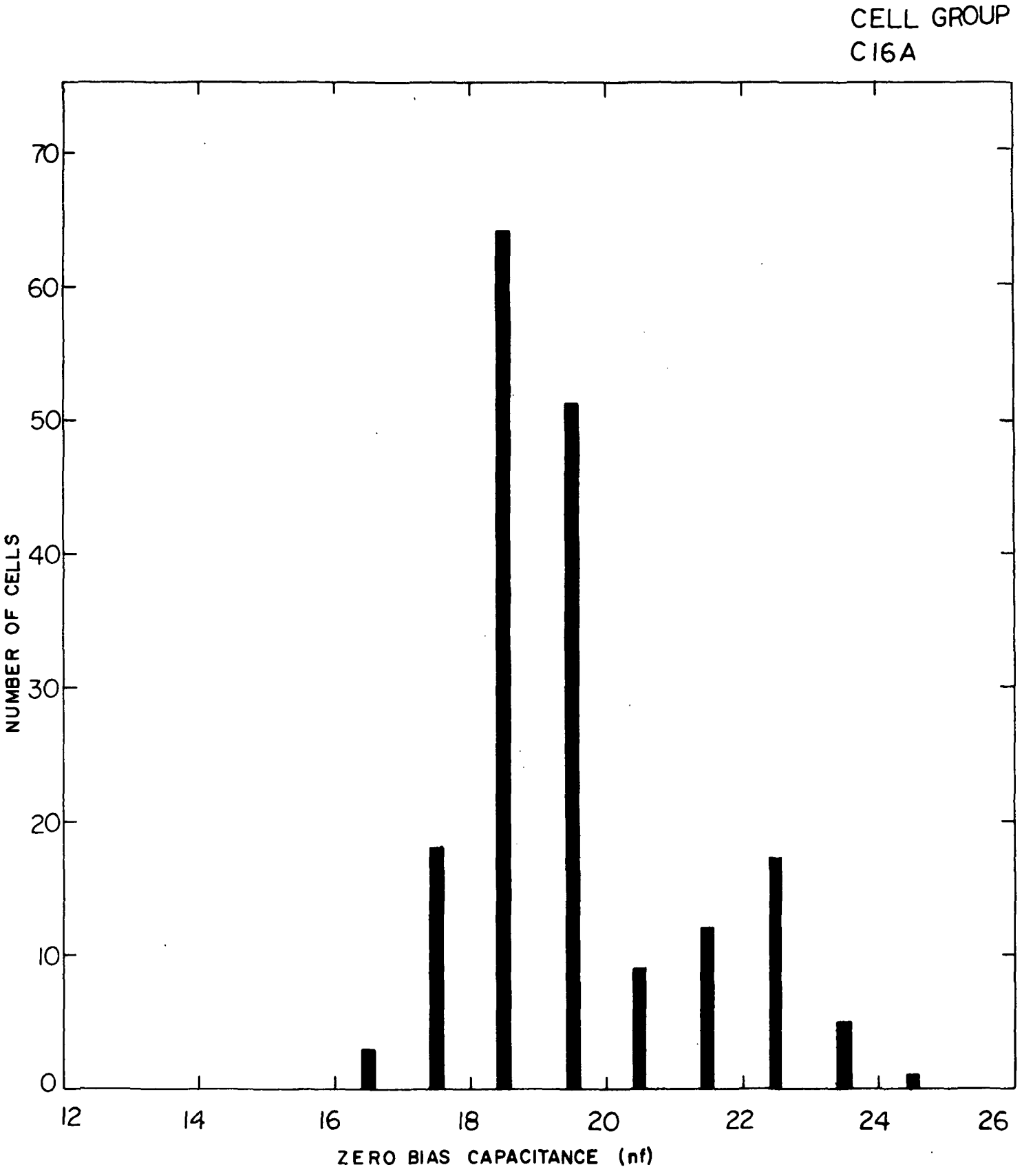

Fig. 20. Capacitance distribution for C-16A

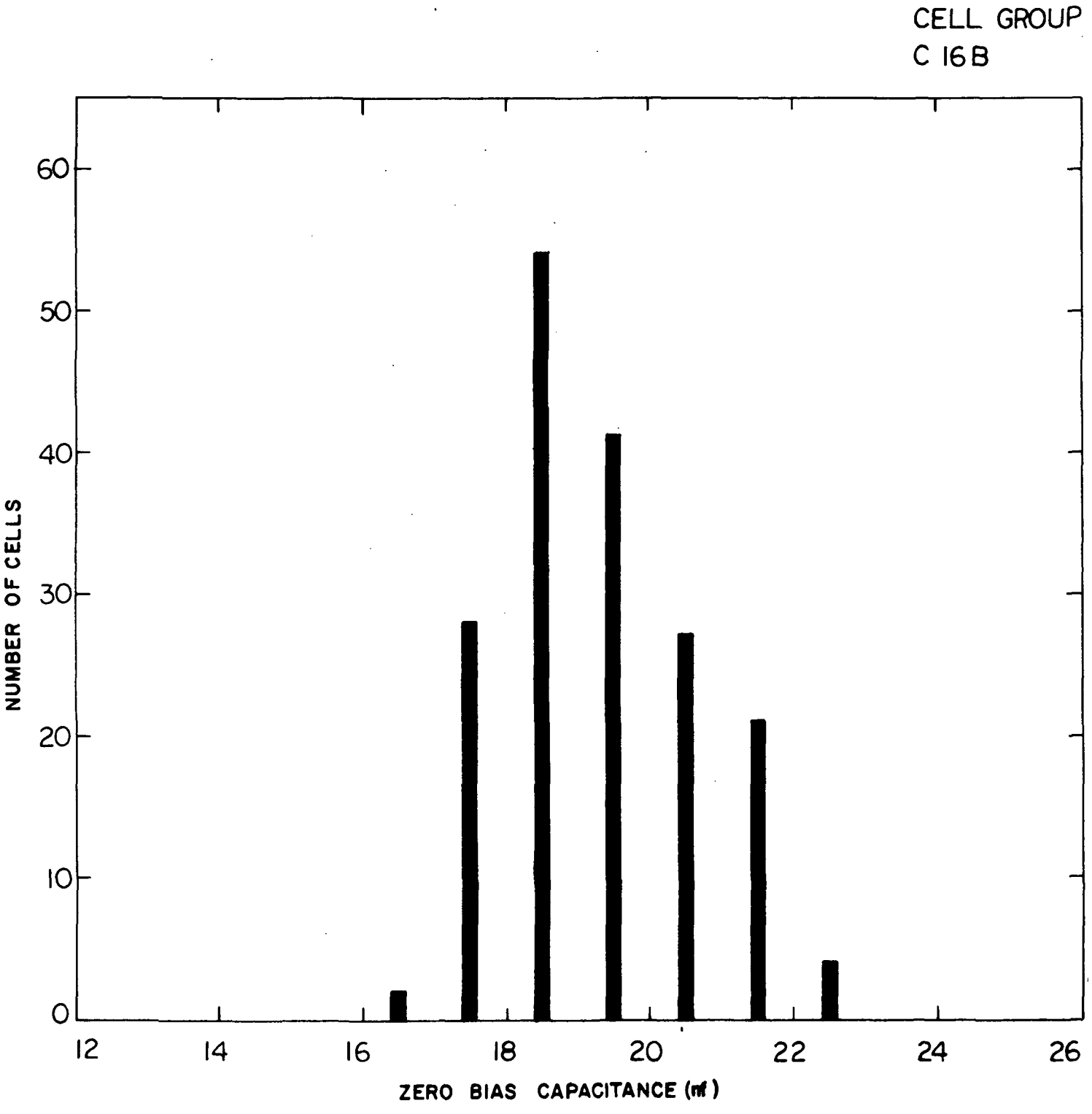

Fig. 21. Capacitance distribution for C-16B

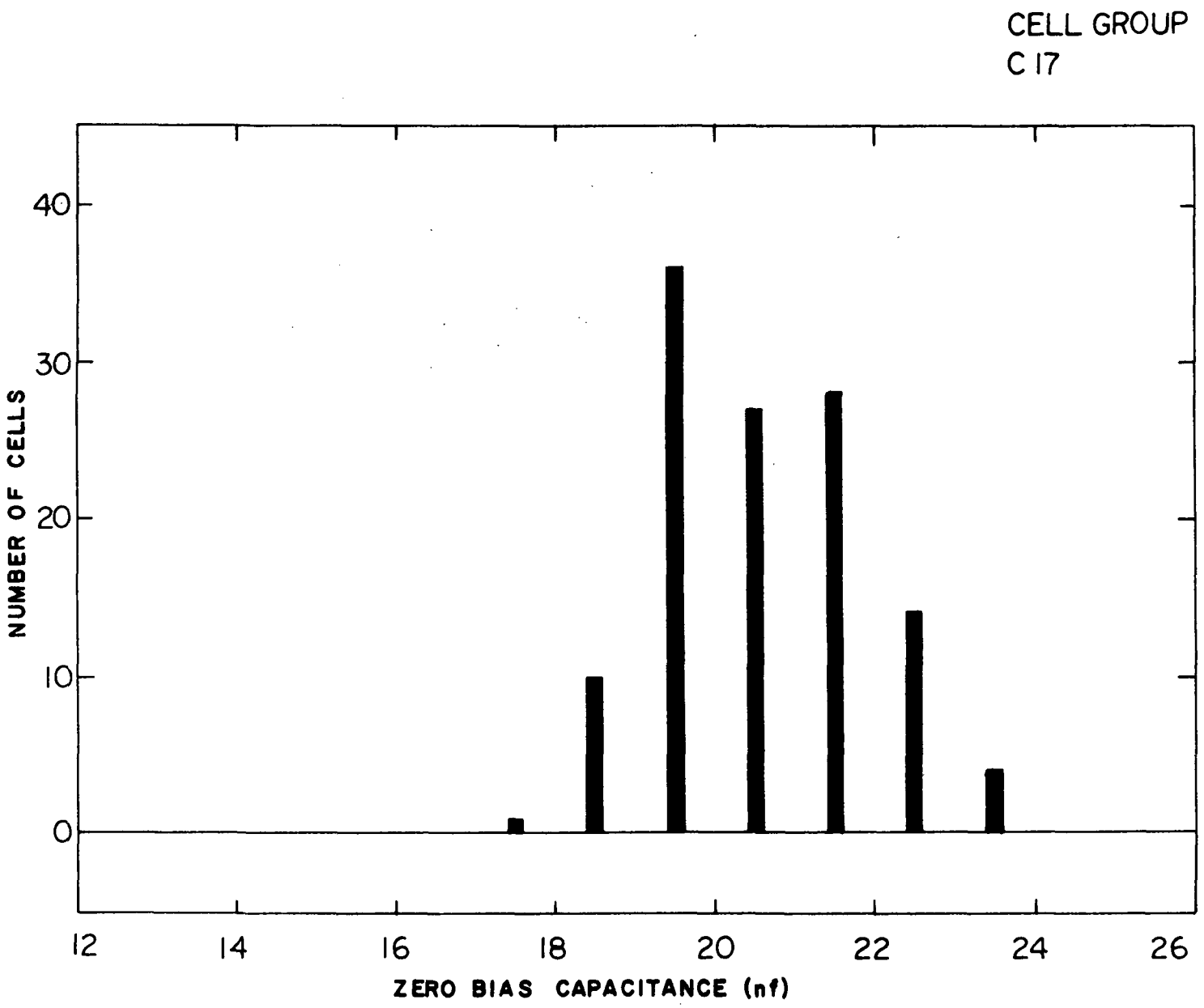

Fig. 22. Capacitance distribution for C-17

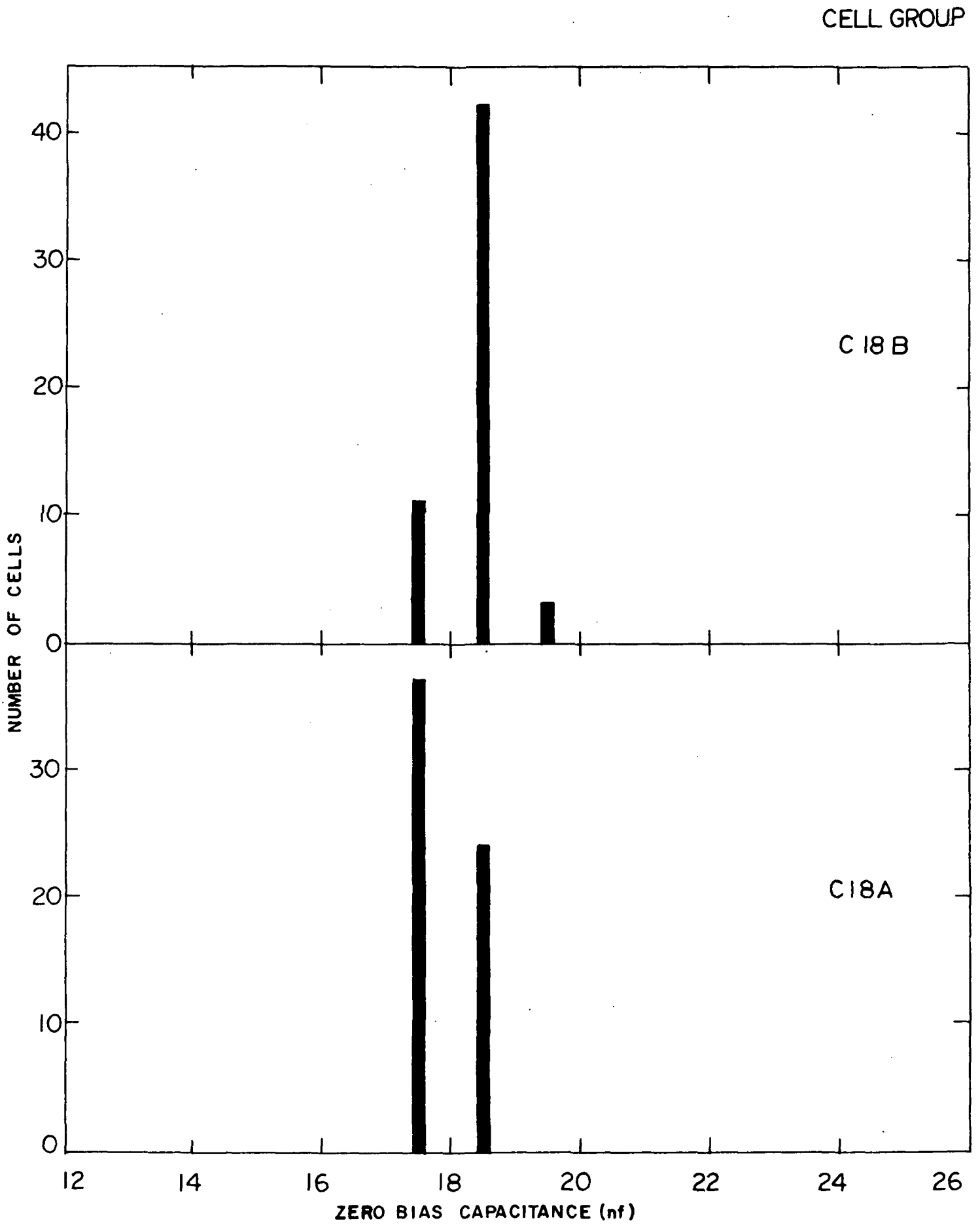

Fig. 23. Capacitance distribution for C-18A, C-18B

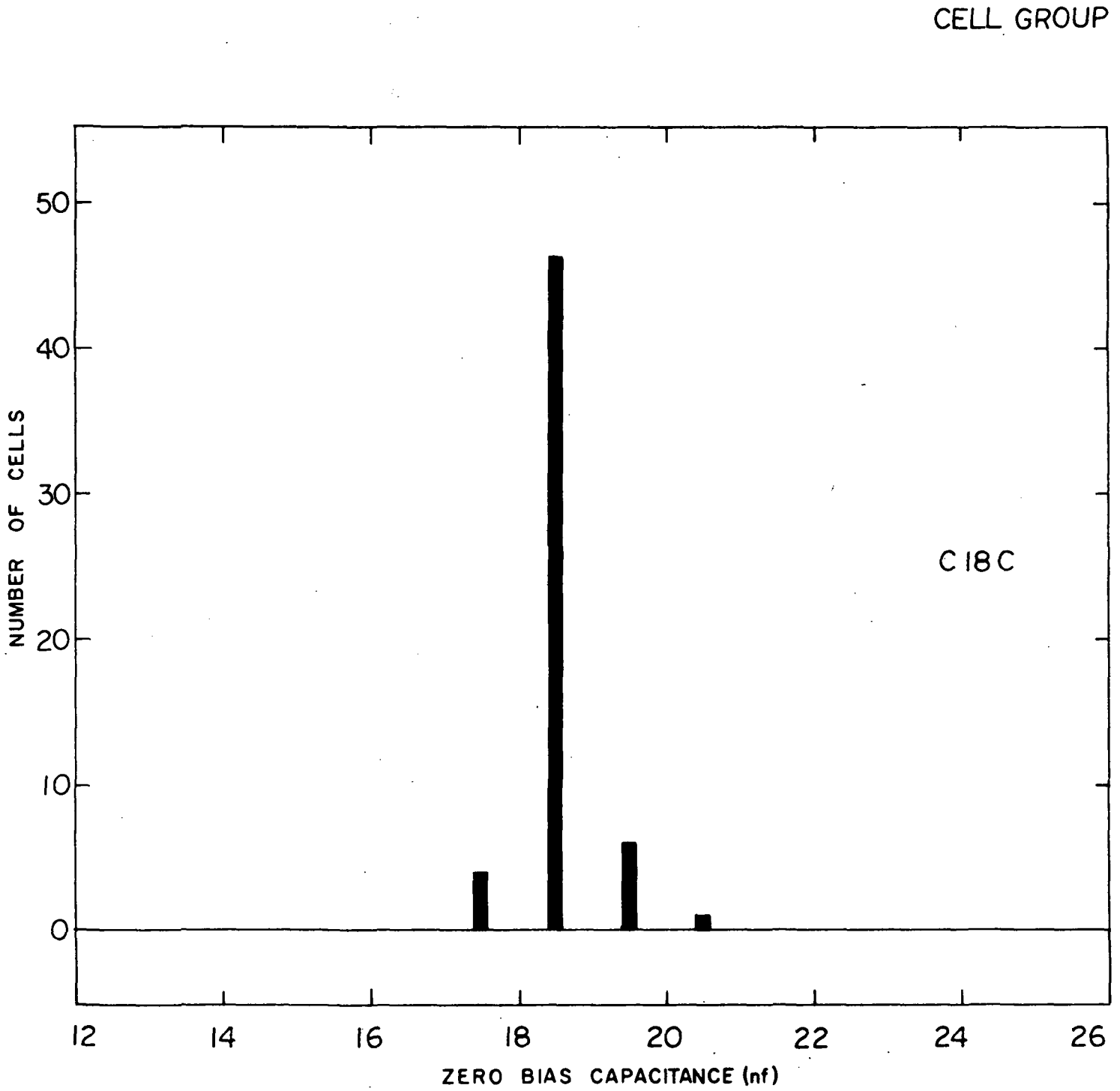

Fig. 24. Capacitance distribution for C-18C

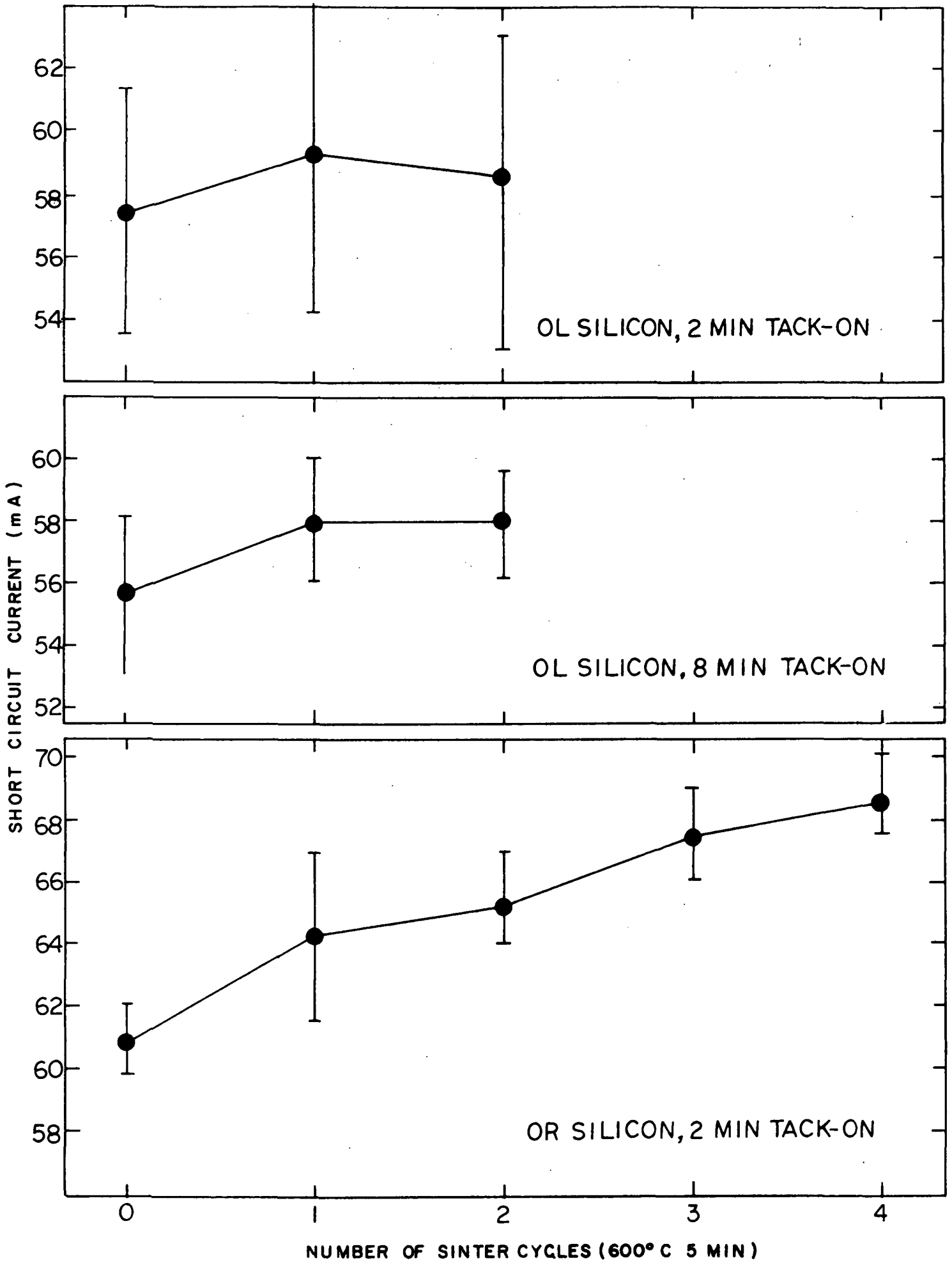

Fig. 25. Changes in I_{sc} during extended sintering

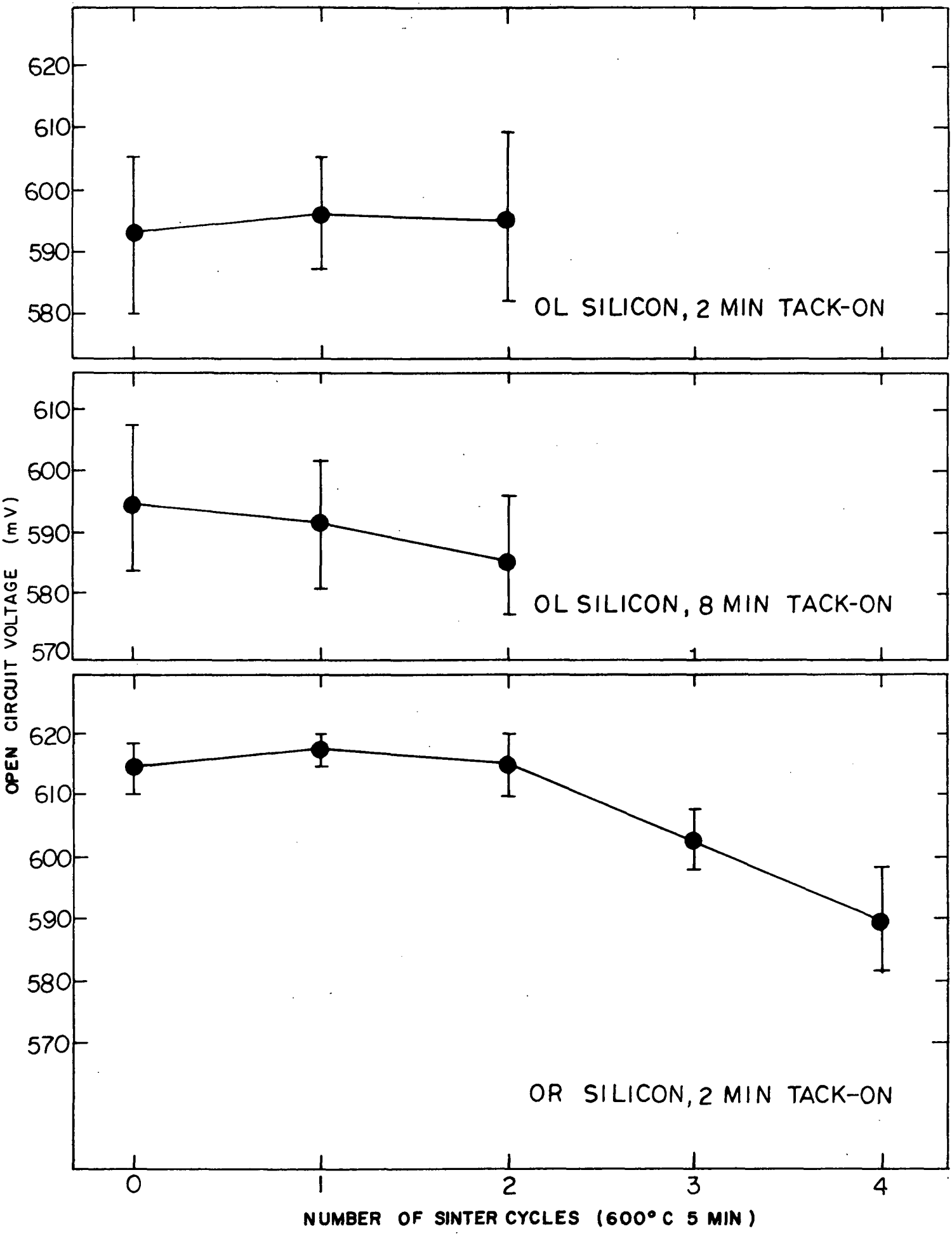

Fig. 26. Changes in V_{oc} during extended sintering

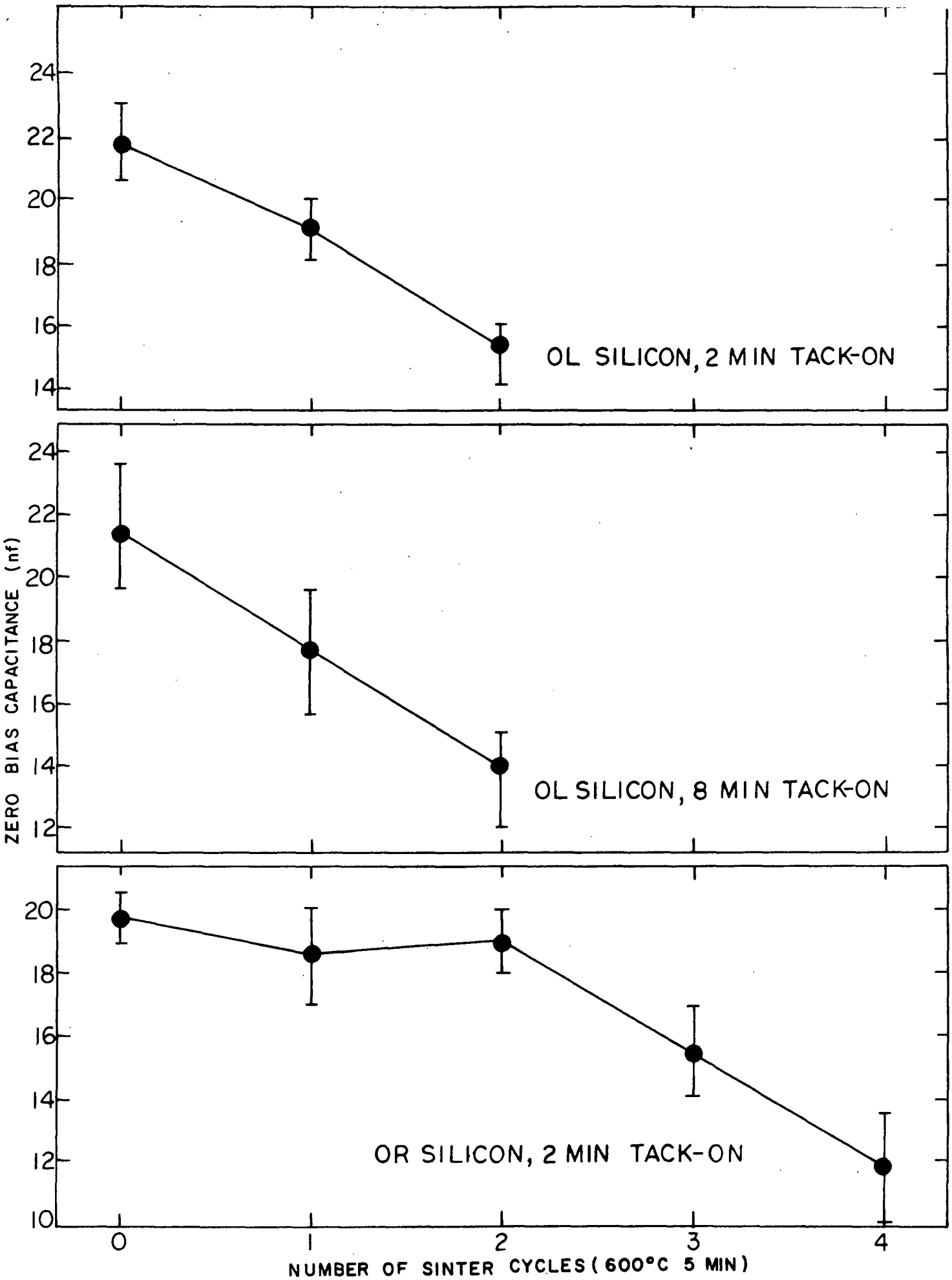

Fig. 27. Changes in capacitance during extended sintering